ACS Catalysis

Review

pubs.acs.org/acscatalysis

Nanoporous Gold as a Platform for a Building Block Catalyst

Arne Wittstock,*[,‡] Andre Wichmann,[†] and Marcus Bäumer*[,†]

[†]Centre for Environmental Research and Sustainable Technology and Institute of Applied and Physical Chemistry, University Bremen, Leobener Strasse NW2, 28359 Bremen, Germany

[‡]Lawrence Livermore National Laboratory, NSCL, 7000 East Avenue, Livermore, California 94550, United States

ABSTRACT: Porous bulk materials are of great interest in catalysis because they can be employed in heterogeneous gas and liquid phase catalysis, electrocatalysis, and in electrocatalytic sensing. Nanoporous gold gained considerable attraction in this context because it is the prime example of a corrosion-derived nanoporous bulk metal. The material was shown to be a very active and selective Au type catalyst for a variety of oxidation reactions. By leveraging the functionalization of the surface of the material with various additives, its catalytic applications can be extended and tuned. In this review, we will summarize recent developments in using nanoporous gold as the platform for the development of high performance catalytic materials by adding metals, metal oxides, and molecular functionalities as building blocks.

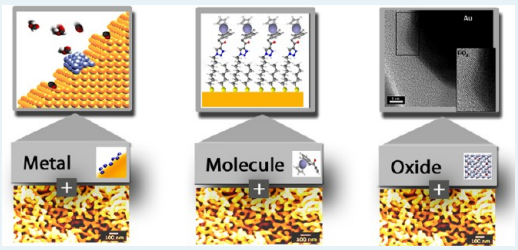

KEYWORDS: *gold catalysis, nanoporous gold, bimetallic catalyst, gas phase catalysis, electrocatalysis, electrocatalytic sensors*

1. INTRODUCTION TO NANOPOROUS GOLD

Nanoporous gold (npAu) consists of a bicontinuous network of Au ligaments and pores and can be described as an open-cell metal foam (Figure 1). This monolithic material is generated by the wet chemical corrosion of an Au alloy containing one or more less-noble metals, such as Ag, Cu, Al, and others.[1] It is thus very similar to Raney type metal catalysts, such as Raney Ni or Raney Cu, which are also prepared by wet chemical corrosion of a precursor alloy.[2−4] Because of the resulting high surface area and catalytic activity, such skeletal catalysts have been employed as versatile catalysts since the early 20th century. In contrast to these materials, npAu does not fracture during the preparation and, thus, stays in its monolithic form. This important characteristic allows for a high electrical and thermal conductivity and opens up applications ranging from heterogeneous catalysis to electrocatalysis, sensors, and actuators.[5−15]

The pores and ligaments of npAu are typically in the range of 30−40 nm and can thus be classified as mesoporous according to IUPAC classification. By a careful choice of the preparation conditions during the corrosion process (e.g. low temperatures), however, the pore sizes can even be decreased to values as small as 5 nm.[16] In this way, very high specific surface areas in the range of 10−15 m^2/g are obtainable.[17] The fraction of the less-noble material in the starting alloy determines the void fraction in the resulting porous network. For Au concentrations above 40 atomic %, the alloy tends to passivate, and no bulk corrosion is achieved. This threshold is dubbed the "parting limit" and represents an upper limit for Au concentration. The lower limit for the Au concentration is determined by the stability of the resulting porous network, which is in the range of 20 atomic % Au. Hence, the void volume of the evolving porous network can be tailored between 60 and 80 %.

First scientific publications studying the corrosion process and nanoporous gold date back to the early 1960s.[18−20] Later, in the context of the evolving nanotechnology in the 1990s and the beginning 2000s, researchers discovered the technological potential of npAu for various applications. Since then, the annual number of publications has been steadily increasing, from 11 publications in the year 2000 to more than 200 publications in the year 2011.[21] The reason for the growing interest can be explained by the comparatively simple and undemanding preparation of the material in conjunction with its structural and chemical flexibility, allowing a broad range of applications (Figure 1). Depending on the dimensions of the starting material, a large variety of sample morphologies and shapes can be realized. Centimeter-sized cubes or cylinders, disks or free-standing membranes with thicknesses of some hundreds of micrometers, or even thin films with thickness as low as 100 nm are available. Independent of the form, all specimens consist of bulk nanostructured gold with pores and ligaments in the size of some tens of nanometers, absolutely homogeneous throughout the entire sample. By leveraging the inherent instability of nanosized structures at higher temperatures, the ligament and pore size of the material can be tuned from about 30 nm all the way up to micrometers, employing thermally activated coalescence of the nanostructure.[22−24] It is noteworthy that the bicontinuous morphology of the material is not altered during this process. Literally, if looking at scanning electron micrographs of these annealed samples, only the scale bar is different. Furthermore, coating techniques and slip-casting allow bringing the relative density of the material down to about 2−3%, equivalent to a material investment that is

Received: April 8, 2012
Revised: July 7, 2012
Published: September 25, 2012

   dx.doi.org/10.1021/cs300231u | ACS Catal. 2012, 2, 2199−2215

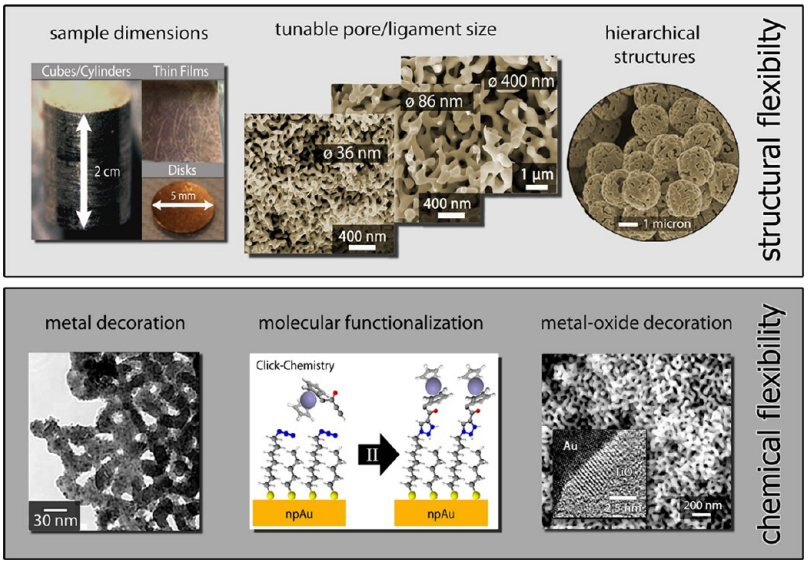

Figure 1. Structural and chemical flexibility of nanoporous Au-based functional materials. Samples with dimensions on the order of centimeters, such as cylinders or cubes, and in the nanometer regime, such as 100-nm-thick films, can be readily prepared; pore and ligament sizes can be tailored between several tens of nanometers up to micrometers. Furthermore, plating techniques open the door to hierarchical structures. Tailoring of the surface chemistry by addition of metals, metal oxides, or organic entities enables applications in sensorics and catalysis. (TEM reproduced from ref 26, copyright Elsevier, 2012).

comparable to supported nanoparticle catalysts.[25] For example, if this material is used in the form of thin films on the order of 100 nm, the amount of Au is less than 0.1 mg/cm^2, a number that is certainly acceptable, for example, in fuel cell applications. Thus, even though npAu is a bulk nanostructured material, the overall material investment of this precious metal can be reduced to competitive and economically viable numbers.

Recent research has impressively revealed that the self-contained nanoporous structure opens the doors for fascinating applications in various fields of catalysis, either using it "as prepared" or after modification with additives, such as metals, metal oxides, or organic entities.[7,26−29] Because of its nanostructure, this material exhibits a very high specific surface area, maximizing the surface-to-volume ratio and the surface area, which is accessible to reactants. Also of advantage is the high electrical and thermal conductivity in conjunction with the well reproducible and tunable monolithic structure. As shown by model studies under ultrahigh vacuum conditions,[30,31] the surface chemistry of Au is very predictable, also meaning minimal degradation due to corrosion or poisoning by sticking of undesired surfactants.

In this Review, we will focus on means to increase the scope of applications by functionalization of npAu with various additives; we will especially highlight options of using the material as a platform for the preparation of novel catalytic materials according to a building block design. (For more detailed information on the catalytic properties of pure npAu, the reader is referred to other recent reviews on this topic. See, e.g.,refs 1, 32.) We will first introduce the material and its catalytic potential. In the following sections, we will describe recent efforts and reports aimed at modifying the surface of the material for applications in gas phase catalysis and electrocatalysis and as electrocatalytic sensors.

1.2. Gold As a Material. Gold as a material has inspired and fascinated mankind ever since ancient times. Historically, it was used and recognized even before other metals, such as bronze or iron.[33] Gold is one of the very few metals that can be found in nature in its metallic form. Its nobleness and resistance to corrosion in conjunction with the apparently immutable shiny yellow color have made it the primary embodiment for eternal wealth, a fact that is well reflected in the increasing interest for gold as a safe investment in economically troubling times.

Certainly, the basic reason making gold a precious and expensive material is its rareness. The average concentration of gold in the earth crust is only 2−5 parts per billion (ppb, weight).[33,34] Interestingly, even these tiny amounts are predominantly not native to earth but are speculated to originate from meteorites that hit the earth about 3.9 million years ago.[35] Mining of gold becomes economically viable only at places where the gold content is enriched by at least a factor of 1000, bringing the concentration of raw gold in the mined material to concentrations of more than 1 ppm. A famous example of such an area is the Whitewatersrand Basin in South Africa. Although the production of gold from this area has been continuously decreasing within the last years, it makes South Africa still the fourth largest producer of gold, excelled only by China (the largest producer), Australia, and the USA. In addition to the mining of gold from natural deposits, the recycling of gold from scrap material has become more and more important. In recent years, countries such as the USA have generated more gold from recycling than from mining.

Perhaps the oldest use of gold is in the form of jewelry and art. Even in our modern times, about half of the production of gold is still used in this way.[36] The second largest fraction (40%) of the gold production goes into monetary assets. Interestingly, only 1/10 of the world's gold production is used for technological purposes, mainly as a conductive material for electronics.

Although it seems that gold has only minor technological importance, it is one of the rising stars in research and new technologies, such as biomedicine, water purification, fuel cells, exhaust gas treatment, energy-efficient glazing, catalysis, and many more.[36] The reason for this is that gold is the prime

example for a nanomaterial that changes its characteristics, such as color or chemical activity, when it is used in a nanosized form.

1.3. Nanotechnology and Gold. Nanotechnology comprises the control and manipulation of matter on the scale of a few atoms and molecules, respectively. The term originates from the prefix "nano", which means a billionth (10^{-9}). One nanometer (nm) is about the size of 4−5 gold atoms in a row. Materials that exhibit characteristic features between ∼1 and 100 nm are dubbed nanomaterials. For the above reasons, modern nanotechnology is strongly dependent on visualization of these small structures by electron microscopy (SEM and TEM) as well as on the controlled modification on the scale of a few atoms, for example by using electron beam lithography or atomic probe techniques.

In some cases, structures can also be formed and controlled on the order of nanometers by self-structurization phenomena, that is, literally by Mother Nature's hands. This is why first reports on the use of corrosion to generate nanoporous gold structures can be dated back to precolumbian civilizations many hundreds of years ago. They used the superficial corrosion of a Au-containing alloy (e.g. Au−Cu) as a means of gilding. The working piece made out of a comparatively cheaper Au alloy was exposed to heat and an oxidizing surrounding. Subsequent burnishing of the superficially dealloyed artwork generated a genuine shiny gold surface. This guilding technique, also called "mis-en-colour", was further used by artisans throughout the following centuries. However, all these artisans were blind to the true nature of the material they were working with. Only after the development of the first electron microscopes in the middle of the most recent century could these gold structures be visualized. The first report on the formation of gold nanostructures during corrosion was published in the 1960s by Pickering and Swann.[20]

Yet, in addition to its use for gilding why is a nanostructure the very key to a technological application, particularly in the context of catalysis? In contrast to bulk materials in which the fraction of surface atoms is on the order of a millionth and less, nanomaterials contain several percent of surface atoms (Figure 2). As a consequence, the properties of nanomaterials are largely determined by their surface atoms. This is important because the electronic structure of these surface atoms is inherently different from their bulk counterparts as a consequence of the reduced number of nearest neighbors. Depending on the local geometry of the atom (i.e., whether it is located at a terrace, a step, or a kink site), the coordination number of the surface atom is 9, 7, or 6, respectively, as compared with 12 in the bulk (in the case of a face-centered cubic lattice, such as in gold).

In the following, we will discuss two consequences of this dominating role of surface atoms. The first one is geometric in nature. Because of the reduced number of nearest neighbors, charge from unsaturated bonds is redistributed into the remaining bonds. This effect, of course, changes the local geometry and bonding situation, and the atoms at or near the surface regroup. The term surface relaxation describes a rearrangement perpendicular to the surface, and the term surface reconstruction describes a rearrangement parallel to the surface. By using scanning probe techniques, such as STM, this reorganization of surface atoms can be visualized. A very beautiful example is the herringbone reconstruction of the Au(111) surface.[38,39] After this reconstruction the surface contains about 4 % more atoms than the bulk, i.e., the average

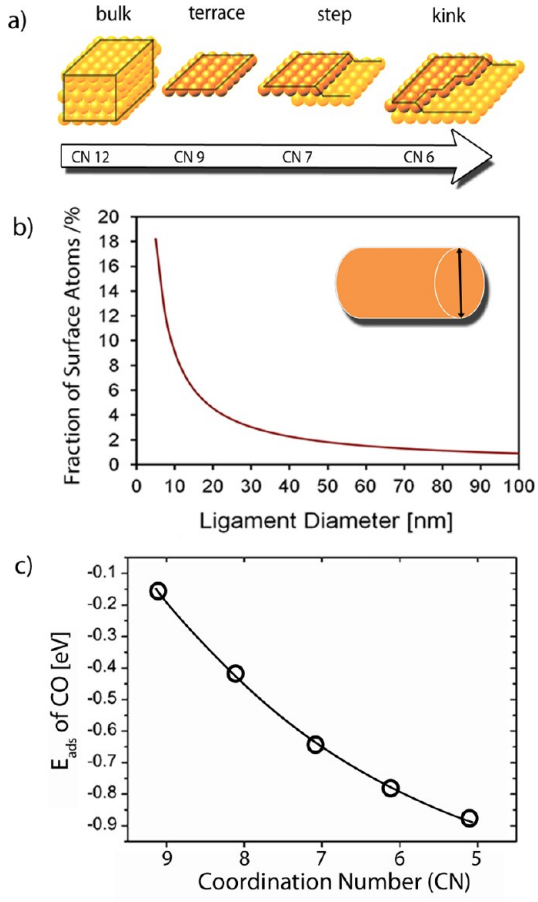

Figure 2. Characteristics of nanomaterials. (a) Surface atoms have a lower number of nearest neighbors (coordination number, CN). (b) When reducing the length, such as the diameter of a ligament or pillar, to only nanometers (1 nm = 10^{-9} m), the proportion of surface atoms reaches several, even tens of percent (calculated on the basis of geometric considerations). (c) The adsorption and bonding of molecules on the surface are a function of the CN and roughness of the surface, respectively. The energy of adsorption (E_{ads}), for example, decreases (stronger bonding) with decreasing CN (calculated for the adsorption of CO on Au(332) and Au(321); based on ref 37, copyright the Royal Society of Chemistry, 2012).

bond length between gold surface atoms is reduced as compared to the bulk. This mismatch of bond length between the surface atoms and the bulk evokes stress, which can be tensile, i.e., the surface is stretched as compared to the bulk, or compressive, meaning that the surface is compressed as compared to the bulk and tends to expand, if allowed.[40] Since nanomaterials consist of a large fraction of surface atoms, this surface stress does impact the entire material. It was shown that, when addressing and altering the surface stress of materials, such as npAu or npPt, by electrochemical or chemical means, the macroscopic dimensions of millimetre sized specimens can be changed even up to fractions of a percent.[6,41−43]

The second consequence is closely related to the chemical and, thus, the catalytic activity of surface atoms and concerns the interaction with adsorbates. For gold, it was found that the desorption energy for a CO molecule adsorbing on the Au surface correlates with the CN of the particular surface atoms. With decreasing coordination, the chemical attraction between the CO molecule and the surface atom increases (Figure 2).

dx.doi.org/10.1021/cs300231u | ACS Catal. 2012, 2, 2199−2215

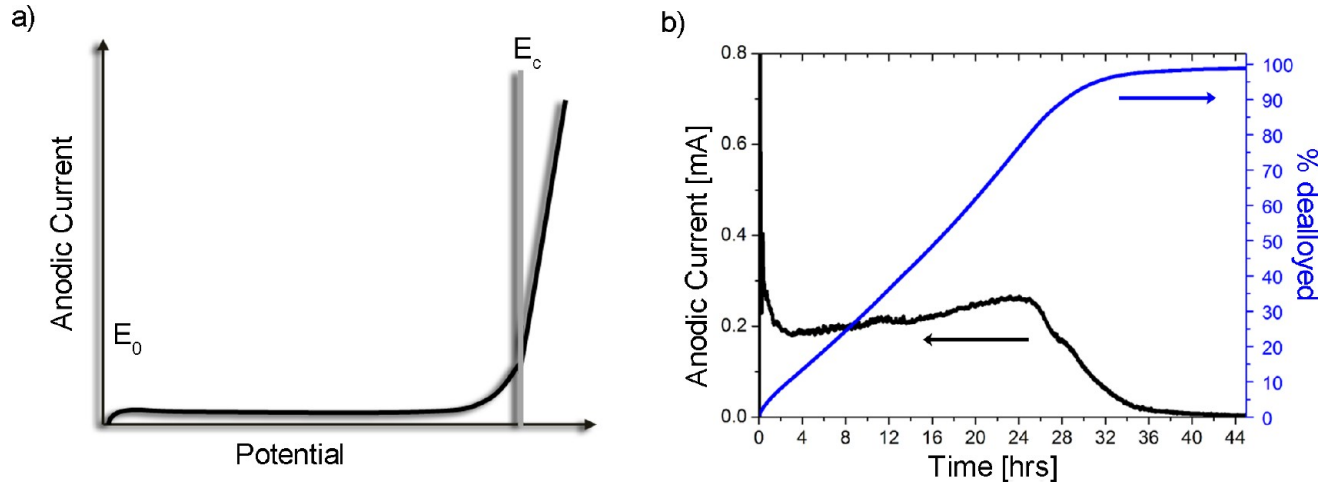

Figure 3. (a) Characteristic run of the anodic current as a function of the applied potential. Above the reversible thermodynamic threshold for corrosion, E_0 (e.g., oxidation/dissolution of Ag), the anodic current remains small at first as a result of a passivation of the alloy surface by Au atoms. Only after reaching the critical potential for bulk corrosion, E_c, does the anodic current steeply increase. (b) Typical evolution of the anodic current during dissolution of Ag from a $Ag_{70}Au_{30}$ alloy in 5 M nitric acid at 60 mV vs a Pt reference (~1200 mV vs NHE under chosen conditions). The anodic current can be transformed into an etching rate. Apparently, after ~32 h, the corrosion of Ag is close to 100%, and the current approaches zero.

Because the interaction with terrace atoms is weak and, thus, the coverage low, low-coordinated Au atoms at steps and kinks are important, for example, for the (low-temperature) oxidation of this molecule, a reaction for which Au is famous.

Nørskov and co-workers investigated and described the adsorption and bonding of a variety of molecules with transition metal surfaces by means of DFT calculation.[44−50] According to their work, the first moment of the distribution of the energy of the d-states, which they dubbed the d-band center, determines the interaction. In the case of a high-lying d-band center, the antibonding states resulting from the interaction of the d-band with the molecular orbitals of the adsorbate are likely to be above the Fermi edge and, thus, unoccupied. The position of the d-band center is not only a function of the atomic number of the metal but also shifts with the coordination number of the surface atoms. For late transition metals, the energy of the d-band tends to shift upward with decreasing coordination number. This effect is strongly pronounced for gold. Because the electron configuration of the ground state of gold is [Xe] $4f^{14}$ $5d^{10}$ $6s^1$, the d-band is completely filled, and the center of the d-band is well below the Fermi level. When forming a bond with an adsorbate, the antibonding state is thus likely to be filled, and the bond formation is unfavorable.[51] Yet, for nanostructures of gold, the position of the d-band of gold is shifted upward, and thus, bond formation becomes more favorable.[46]

1.4. Generation of Nanoporous Gold. The generation of npAu is based on the electrochemical corrosion of a Au alloy containing one or more less-noble constituents. For this reason, this process was dubbed dealloying. Prominent starting alloys are Au−Ag,[18,52] Au−Cu,[53,54] Au−Ni,[55], and Au−Al,[56,57] as well as ternary alloys such as Au−Ag(Pt).[58] More recently, multicomponent bulk metallic glasses have also been used.[59,60] In all these cases, a nanoporous gold material can be obtained, differing though, with respect to porosity and composition, owing to differences in the phase diagrams, differences in lattice constants of the alloy constituents, or the different tendencies to passivate during dealloying.[53,56,57] It is noteworthy that Au and Ag both have fcc structures and form a homogeneous solid solution, regardless of their composition. Accordingly, corresponding alloys have proved to be particularly suitable because they can be dealloyed to >99%[5,33] (Figure 3), and the resulting porous structure of the npAu is uniform throughout the material (Figure 1).

A viable precursor alloy can be prepared by melting the correct amounts of Au and Ag at sufficiently high temperatures (i.e., 1100 °C). After casting and cooling of the alloy, the material can be further processed, that is, cut and rolled into the desired shape. One crucial factor for the homogeneity of the porous structure is the annealing after casting and mechanical treatment of the material at sufficiently high temperatures (e.g., 875 °C under Ar atmosphere). For millimeter-sized specimens, this procedure should be run for several days (e.g., 6 days) until the formation of large crystallites, preferably several tens of micrometers in size, is detectable.

It turns out that two parameters are crucial for a successful dealloying: the parting limit[61,62] and the critical potential (E_c).[63−65] The fact that only alloys containing less than ~45 at. % of Au can be successfully dealloyed is a consequence of this parting limit. This phenomenon can be understood in terms of a coordination effect: above a critical concentration, the less-noble metal atoms (Ag, Cu) are shielded and passivated, respectively, by Au atoms. Artymowicz et al. recently presented a kinetic Monte Carlo simulation, including the percolation theory.[66] The authors show that the coordination threshold of 9 Ag atoms leads to the experimentally found parting limit of ~55 at. % Ag.

Another parameter that is important for dealloying is the so-called critical potential (E_c), which is a consequence of the well-known overpotential in electrochemistry (Figure 3). The Nernst potential as described by thermodynamics does not suffice to induce bulk corrosion. Only at a potential usually some hundred millivolts higher than the thermodynamic threshold does the current resulting from the dissolution of Ag atoms rapidly increase. Investigation of the alloy surface showed that below the critical potential, E_c, the resulting surface is smooth and enriched in Au, pointing toward a passivation of the surface due to slow kinetics of Au diffusion.[20,67] The critical

potential depends on the composition of the starting alloy, the electrolyte, and further additives, such as halides.[63−65]

An important contribution for helping to understand the formation of npAu was the surface-diffusion-based model developed by Erlebacher and co-workers that is able to reproduce the early stages of the formation of the characteristic 3D morphology of npAu.[8,68,69] This model is based on three competing processes: the electrochemical dissolution of the less-noble constituent (Ag), surface diffusion of the noble constituent (Au), and capillary action.[8,69] Although the Ag atoms are dissolved in a layer-by-layer fashion, the gold atoms can diffuse along the surface and form islands. Further dissolution of Ag atoms leads to erosion of islands so that ligaments are formed. Because of capillary action, the initially formed ligaments coarsen, thus exposing residual silver. Kolluri and Demkovicz recently reported on an atomistic model capturing further stages of the formation of the ligaments of npAu by coarsening of the initial ligament network.[70] Plastic deformation of the initial ligaments by collapsing onto each other drives the coarsening and explains experimental findings, such as the minimal ligament diameter of ∼5 nm or the observation of voids inside the ligaments.[71]

Basically, one can distinguish two means of corrosion: the *free corrosion* and the corrosion in an electrochemical cell, either in a *galvanostatic* or *potentiostatic* manner. In the case of free corrosion, the working piece is simply submersed in an electrolyte such as concentrated nitric acid. The open circuit potential drives the dissolution of the less noble material (the reduction of nitrate constitutes the necessary cathodic reaction). Free corrosion can be performed at room temperature or even at 0 °C in the case of Ag or at slightly elevated temperatures of 40 °C and above in the case of Cu and Al.[53,56] This rather simple means of preparation works for thin films on the order of 100 nm up to centimeter-sized cubes or cylinders. In the case of thin films adhered to a substrate, buildup of stress might lead to cracking. Sun and Balk proposed a two-step dealloying approach reducing the overall shrinkage.[72] For larger pieces, such as millimeter-sized cubes or disks of $Au_{30}Ag_{70}$, alloy shrinkage is typically below 1% of the edge length and hardly observable.

The second route is dealloying in an electrochemical cell (e.g., *potentiostatic corrosion*) by applying a sufficiently positive potential to the alloy, initiating corrosion. Typically, a three-electrode setup is used, with the alloy piece as the working electrode, a reference electrode, plus a counter electrode (e.g., a Pt plate). The most commonly used electrolyte is $HClO_4$, with concentrations between 0.7 and 1 M.[73,74] Another suitable electrolyte is diluted nitric acid, for example, with a concentration of 5 M,[32] or neutral Ag nitrate solution.[75] The potentiostatic corrosion requires a more sophisticated setup (including a potentiostat) than the free corrosion, but it provides better control over the corrosion process. For example, by applying a slightly higher potential than the critical potential, Ag is removed very slowly, resulting in mostly crack- and stress-free npAu films.[73] At potentials close to the critical potential, the corrosion rate is very small, typically in the range of microamperes per square centimeter.[63] At higher potentials, the corrosion is greatly accelerated by about 1 order of magnitude (cf. Figure 3), reducing the processing time. Especially, the high corrosion rate at the very beginning of the dealloying is assumed to induce mechanical stress and the formation of cracks; Okman et al. proposed a stepwise increase in the dealloying potential to solve this issue.[76] For potentials close to the oxidation threshold of Au, smaller ligament and pore sizes are also observed, owing to a reduced surface self-diffusion of the Au atoms at this stage.[17] Controlling the potential allows adjusting the dealloying time, the residual Ag, the stress state of the material, and the pore size.

2. CATALYSIS BY NANOPOROUS GOLD

The starting point for the catalytic cycle is the adsorption, or more precisely, the chemisorption, of one or more reactants on the catalyst surface. The catalyst then provides an alternative reaction mechanism with a lower activation barrier and, thus, higher turnover at lower temperature. In a general picture, a strong bonding of the educts results in a lower activation barrier for the particular reaction (Bell−Evans−Polanyi principle); however, a too strong bonding will also impede a high turnover because the molecules do not desorb quickly enough from the catalyst surface. As in the case of the transition metals, the heat of adsorption tends to decrease with increasing atomic number from left to right in the periodic table. The catalytic activity should reach a maximum for elements in the center of the periodic table. The trend was described as the volcano curve and, indeed, many of the highly active metals can be found in groups 8−10 of the transition metals (Fe, Co, Ni, Pd, Pt).[146]

Although Au is located right next to Pt, which is one of the most active transition metal catalysts, its activity seems far inferior. The reason is that flat gold surfaces are distinguished by their weak interaction with most adsorbates.[51] Accordingly, Au was considered "catalytically dead" for a very long time. The reports from the group of Bond in the 1970s[77] on olefin hydrogenation and later in the mid-1980s from the groups of Haruta[78] and Hutchings[79] for the CO oxidation and the olefin chlorination, respectively, impressively revealed, however, the catalytic potential of gold. The very key to its activity is the dispersion of small Au particles in the size of a few nanometers on a suitable oxidic support. Although controversially discussed throughout the last two decades, it appears that especially the activation of molecular oxygen profits from a synergistic effect at the interface between the gold particles and the support.[80−82]

The report of the catalytic activity of nanoporous gold in 2006 by Zielasek et al.[83] and shortly after by Ding et al.[84] came as a bit of surprise because this material does not contain any oxidic support. Consequently, studies focused on the material because it appeared that it might reveal the genuine catalytic properties of *unsupported* gold, just originating from its nanostructure.[7,85] Later studies also included potential partners of gold, such as traces of the less noble metals (Cu, Ag), which can remain in the material after dealloying.[86] Although the quantity of the residual metal, such as Ag, is well below 1 at %, it can enrich at the surface and contribute to the catalytic activity, especially with respect to the activation of molecular oxygen.[37,87−89]

Of course, it has to be kept in mind that the origin of the catalytic activity and the active state of the catalysts surface may very well be a function of the surrounding medium, as well, which is, of course, different in the gas phase in comparison with reactions in the liquid phase. In the latter case, the surface chemistry and the underlying mechanism are mostly distinguished from the gas phase by a higher concentration of spectator species on the surface. For example, although water can be exploited as a solvent and oxidant in the liquid phase for the oxidation of silanes,[90] its role in the oxidation of CO in the gas phase is very different. Even though it was found to be beneficial for the catalytic activity when in the form of moisture,

dx.doi.org/10.1021/cs300231u | ACS Catal. 2012, 2, 2199−2215

it cannot be used as the oxidant, replacing O_2.[32] Despite potential contributions from residual components in the material or an influence of the reaction environment, the catalytic activity and, especially, the selectivity of this unsupported gold catalyst can be understood and described according to the surface chemistry of Au. This is exemplified by the activity for CO oxidation at temperatures below 0° and the highly selective oxidation of alcohols (Figure 4).

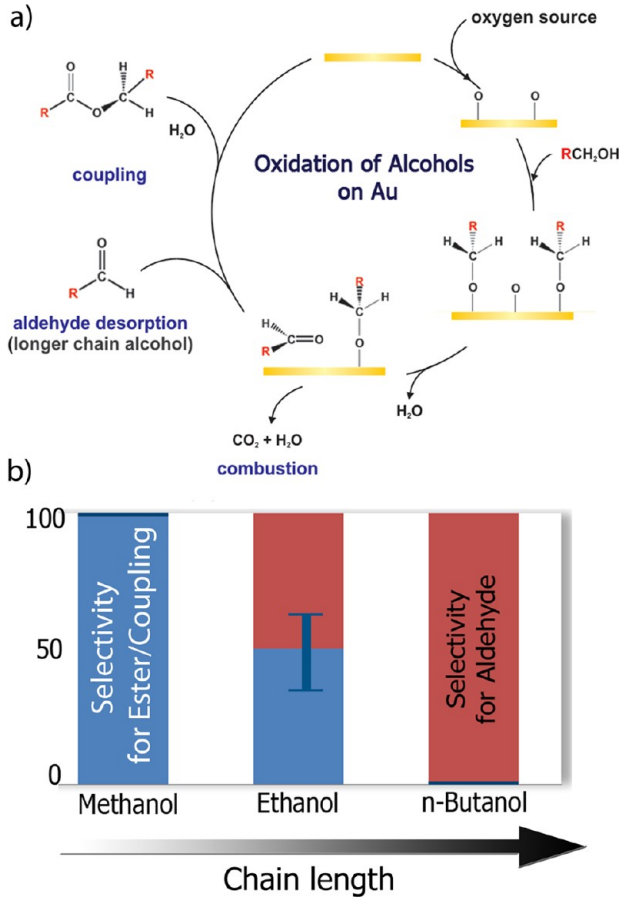

Figure 4. (a) Molecular transformation of primary alcohols on npAu in the presence of reactive oxygen.[5,92−96] (b) The selectivity with respect to either the formation of the ester (coupling) or the aldehyde was found to be a function of the chain length of the alcohol (reproduced from ref 92, copyright John Wiley and Sons, 2012).

Very much in contrast to the previous belief of gold as being catalytically dead, it appears to be right at the pinnacle of the volcano curve, showing even higher activity for oxidation reactions than platinum.[91] It is the noble character of gold and the weak interaction that brings about the activity at very mild conditions, making it a very "green" catalyst. The low concentration of adsorbates also at ambient pressure conditions renders gold a very "predictable" catalyst as well. In the case of unsupported npAu, studies showed that insights on the molecular transformation of reactants as derived from model experiments under UHV conditions can be directly transferred to npAu working at ambient pressures[5,92]

For example, the aerobic oxidation of primary alcohols, such as methanol, ethanol, and *n*-butyl alcohol, is already catalyzed by npAu at temperatures as low as 20 °C with considerable yields.[5,92] The origin of the catalytic activity of the gold is reactive atomic oxygen adsorbed on its surface.[97] It initiates the catalytic cycle by reaction with the alcoholic proton in a Brønstedt acid−base type reaction.[95,96] The resulting alkoxy group is bonded to the surface and can undergo further β-hydrogen abstraction, resulting in the particular aldehyde (Figure 4). The selectivity of the catalytic reaction is governed by the activation energy for β-hydrogen abstraction, resulting in the aldehyde, which can either desorb from the surface or react with an adjacent alkoxy moiety, forming the ester. Interestingly, this activation barrier is a function of the carbon chain length of the alcohol, decreasing from methanol to ethanol to *n*-butyl alcohol.[94] Accordingly, the selectivity of the reaction at ambient pressure when using npAu catalysts was found to shift from the exclusive formation of the ester in the case of methanol toward the exclusive formation of the aldehyde in the case of *n*-butyl alcohol, with an intermediate situation of ∼50% conversion into both products in the case of ethanol oxidation (Figure 4).[92] In 2010, Ding et al. also reported that larger alcohols, such as benzyl alcohol, can be selectively oxidized using npAu catalysts and O_2 as the oxidant.[98] The main product was the industrially important benzaldehyde; in all cases, the selectivity of the conversion was above 92%; the conversion started at temperatures slightly above 200 °C and already at 240 °C, the conversion was close to 60%, showing a remarkable activity (turnover frequency of ∼1.4 s^{-1}).

In addition to these interesting applications of npAu as a catalyst in the gas phase, its potential was also demonstrated in liquid phase catalysis. For example, glucose can be selectively oxidized to gluconic acid, employing npAu catalyst at temperatures starting at 30 °C and using molecular oxygen as the oxidant:[13]

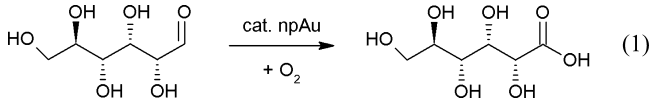

(1)

The reaction conditions were found to be optimal at pH 9 and a temperature of ∼60 °C. Importantly, the catalyst could be recycled several times without apparent loss of activity. But not only carbon based compounds can be oxidized using npAu: Asao et al. demonstrated the selective oxidation of organosilanes into the corresponding silanols in water.[90] The authors used 40 μm thin nanoporous gold foil in the liquid phase to oxidize various organosilanes. Giving just one example, dimethylphenylsilanol was derived within 1 h at room temperature with nearly 100% yield by using finely dispersed 1 mol % of npAu as a catalyst:

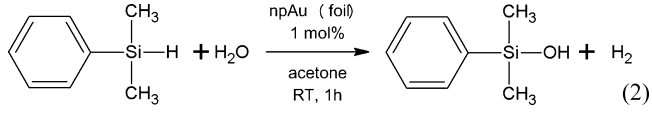

(2)

The turnover frequency for this reaction was calculated to be ∼3 s^{-1}. Also in this case, the npAu catalyst could be recycled and reused several (i.e., more than 5) times. It is the remarkable recyclability of the catalyst in conjunction with the stable catalytic activity that makes this npAu such an interesting material for selective (aerobic) oxidation reactions in the liquid phase.

3. COMBINING NANOPOROUS GOLD WITH OTHER METALS

Although the surface chemistry and catalysis of gold leads to impressive activity and selectivity for many chemical reactions,

dx.doi.org/10.1021/cs300231u | ACS Catal. 2012, 2, 2199−2215

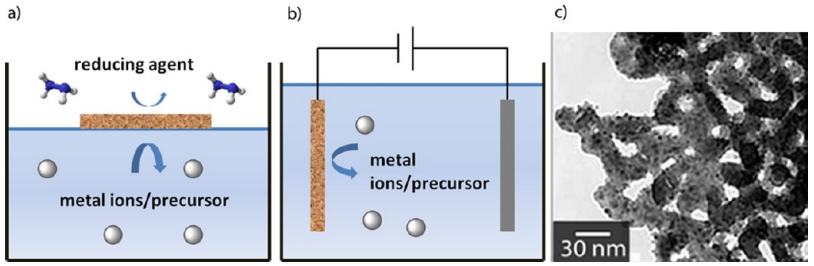

Figure 5. Deposition of metals by chemical reduction of metal precursors/ions from the liquid phase. (a) Chemical reduction at the vapor/liquid interphase, (b) electrochemical reduction, and (c) transmission electron micrograph of a Pt−npAu composite material prepared by chemical reduction of a Pt salt using hydrazine vapor. The resulting Pt particles are finely dispersed on the Au substrate and have an average size of 3 nm, (reproduced from ref 26, copyright Elsevier, 2012).

its activity, for example, with respect to the oxygen reduction reaction (ORR), which is of critical importance in energy related electrochemical applications such as in fuel cells, is inferior to highly active metals, such as Pt. It is thus tempting to alter and tune the surface chemistry of gold by depositing metals such as Pt, Pd, or Ni onto the npAu backbone. The perspective here is 2-fold: on one hand, npAu will provide high electrical and thermal conductivity in conjunction with a very high specific surface area; on the other hand, the catalytic activity of a bimetallic system often proves superior because of a synergistic effect of both metals at the surface, resulting in a unique catalytic system.

In the following, we will focus on the modification of npAu by Pt and its applications in liquid phase electrocatalysis, with the emphasis on fuel cells because Pt is the most prominent and reactive metal in this context. In addition, we will discuss the use of this material combination for sensor applications, taking the electrochemical detection of glucose as an example.

3.1. Deposition of Metals Inside the npAu Structure.

Although it is possible to dealloy trimetallic Au alloys, such as Au−Ag(Pt),[58] resulting in bimetallic nanoporous Au−Pt structures, it is economically more favorable to deposit the expensive metal Pt (or Pd) after the formation of the porous network. In general, one can distinguish deposition of metals from the gas phase by physical or chemical vapor deposition and liquid phase deposition by reduction of a metal salt from solution. In all cases, the high aspect ratio of the pores (i.e., the ratio of the length of the pore and the pore diameter) is a major impediment for uniform and homogeneous coatings of the interior of the porous structure. Techniques such as vapor deposition, comprising evaporation of the metal and subsequent deposition on the porous sample, will inherently suffer from poor conformity of the coating, predominantly leading to a coating of the outer surface of the material. More sophisticated techniques, such as chemical vapor deposition and especially atomic layer deposition (ALD), proved to be advantageous for uniform coatings inside high-aspect-ratio materials, as shown for carbon aerogels with pores in the range of some tens of nanometers, which could be coated with Pt using a well-established ALD routine.[99] Recent work on the deposition of metal oxides inside nanoporous gold structures using this technique will be discussed later in the appropriate section. An experimentally more facile way of depositing metals uses the reduction of a metal precursor from a surrounding solution by (electro-)chemical means (Figure 5).

The group of Erlebacher et al. developed an electroless plating routine floating thin (i.e., ∼100 nm thick) npAu sheets (prepared from 12 karat American white gold leaf) on a water surface containing the particular metal salts and the reducing agent (e.g., hydrazine) in the vapor phase.[100] By separating the two reactants in this way, the reduction proceeds primarily at the gas−liquid interface and inside the pore volume of the npAu sheet, respectively, thus repressing deposition of the metal on the outer surface. The deposited amount of metal inside the pores can be controlled by removal of the reducing agent at some stage and thus ceasing the reaction. Using $Na_2Pt(OH)_6$ as a precursor salt and hydrazine as a reducing agent, a homogeneous coating with Pt particles inside the npAu structure was obtained after less than 3 h of reaction (cf. Figure 5).[100] The Pt particles grew epitaxially on the Au substrate and showed a narrow size distribution between 2 and 4 nm. The fact that the Pt lattice adapted the slightly larger lattice spacing of the Au substrate indicates strong bonding between the Pt and the Au substrate.[101] By using this deposition technique, many different metals, such as Pt, Pd, Ag, Sn, or even metal oxides such as MnO_2, can be deposited inside the nanoporous structure.[7]

A further electrochemical technique to obtain uniform coatings inside the nanoporous structure is underpotential deposition (UPD) (Figures 5b and 6a). By definition, the term UPD denotes deposition of approximately one monolayer of a dissimilar metal A on a metal substrate B at an electrochemical potential more positive/anodic than required for bulk deposition of A.[102] At this potential, the deposition of (sub-)monolayer amounts of the ad-metal is thermodynamically favored, for the interaction between the ad-metal A and the substrate B is more favorable than the interaction of A and A. Because this method is equivalent to the atomic layer deposition mentioned above, it is also referred to as electrochemical atomic layer deposition. Typical ad-metals that can be deposited on Au substrates are Zn, Ag, Cu, Pb, and Hg; the success and the conformity of the deposited ad-layer, however, strongly depends on the choice of electrolyte, the metal precursor (salt), and the pH.[102−104]

Huang et al. investigated the deposition of Zn on npAu substrates using UPD and the subsequent galvanic replacement of the Zn by the more noble Ni metal.[105] The npAu substrate was first submersed in a 0.1 M $NaClO_4$ electrolyte containing 30 mM $Zn(ClO_4)_2$. At a potential of −394 mV and −307 mV vs SCE (saturated calomel electrode), stripping of about 1 ML of Zn onto the npAu substrate was observed. In a second step, the first deposited layer of Zn was replaced by Ni by submersing the sample in a 50 mM $NiSO_4$ solution for 3 min. The resulting Ni−npAu electrode was tested for oxidation reactions, such as glucose oxidation, and showed about 60 times

dx.doi.org/10.1021/cs300231u | ACS Catal. 2012, 2, 2199−2215

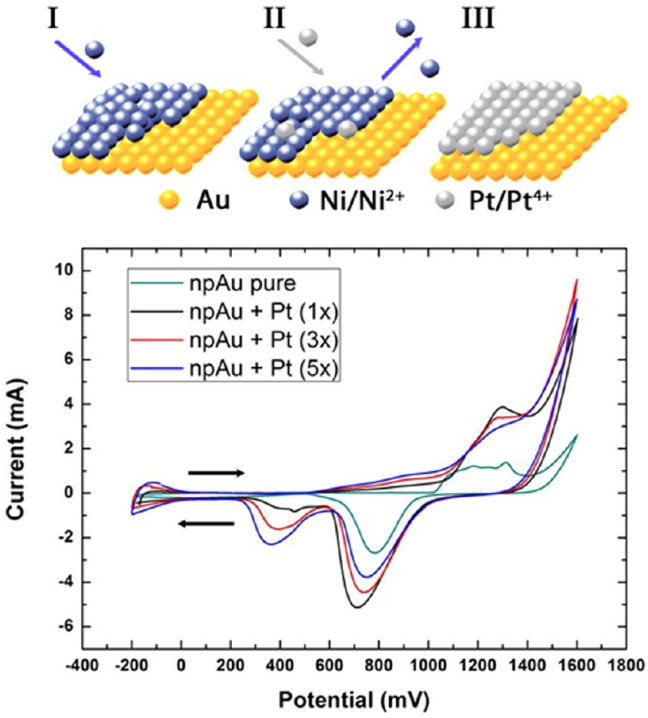

Figure 6. Electrochemical modification of npAu. Upper section: At first, a sacrificial Ni layer can be deposited in a very controlled fashion which is subsequently replaced by Pt by galvanic replacement. Lower section: Cyclovoltammograms after each cycle of Pt deposition onto a npAu electrode. First, the surface of the npAu electrode was cleaned by cycling the sample in 0.1 M sulfuric acid (green line; no Pt-signal at ~400 mV). Subsequently, Ni was deposited by stripping of Ni from a 10 mM $NiSO_4$ solution at a potential of −0.9 V vs Ag/AgCl for 60 s. The sample was subsequently immersed in a 10 mM H_2PtCl_6 solution for 3 min. Cyclovoltammograms of the resulting electrodes for various repetitions of this procedure are displayed. After five iterations, the signal intensity saturates, indicating complete exchange of the Ni by Pt. (conditions: npAu disk: 5 mm diameter and 250 μm thick; 50 mmol H_2SO_4; Ag/AgCl reference electrode; sweep velocity of 1 mV/s).[107]

increased activity as compared with a bare npAu electrode and a larger potential window for electro-oxidation.[105]

In a separate study, Rettew et al. investigated the replacement of sacrificial Ni layers deposited on flat and single crystalline Au substrates that were subsequently replaced by Pt by galvanic exchange-reaction (Figure 6).[106] So far, many studies have focused on the deposition of, for example, Cu as the first sacrificial layer due to its advantageous UPD properties; however, Ni can be overpotentially deposited in a very controlled fashion, and it is less noble than Cu, so it can be replaced by metals such as Mo, Sn, and Pb in the subsequent galvanic reaction, which would not be possible using Cu for its electrochemical nobility. To demonstrate the feasibility of this approach even for highly porous electrode materials, a npAu membrane (diameter of 5 mm and thickness of 250 μm) was decorated with Pt following Ni deposition according to the procedure described in ref 106 (cf. Figure 6).[107]

3.2. Applications in Fuel Cells. Fuel cells are electrochemical devices generating electricity from a chemical (redox) reaction. Prominent examples are the so-called polymeric-electrolyte- or proton-exchange membrane fuel cells (PEMFC).[108] For low-temperature applications (i.e., below 100 °C), H_2-PEMFCs as well as direct methanol fuel cells and direct formic acid fuel cells (DFAFC) have been widely investigated.[108] While for all of these cells, oxygen is reduced on the cathode side of the cell (ORR), and the anodic oxidation reaction is based on the splitting and oxidation of the particular fuel (H_2, methanol, formic acid). Pt is typically employed as the catalytically most suitable metal on both electrodes, finely dispersed on a conductive support. Carbon type supports (carbon black, activated carbon, or carbon aerogels[99,109]) are preferable in terms of their economic viability and the low cost of carbon as a resource. Fast degradation of carbon based systems due to a lack of chemical interaction of the Pt particles with the carbon support as well as corrosion and fast contamination of the carbon support inspired further research on alternative strategies.

Interestingly, Pt−npAu as a highly conductive, durable, and active electrode material −profiting from a bimetallic effect enhancing the catalytic activity - can achieve economic viability when in the form of very thin films requiring less than 0.1 mg of Au and 50 μg of finely dispersed Pt per cm^2.[26] In the following, we will report on Pt decorated npAu electrode materials with respect to the oxidation of H_2, methanol and formic acid, respectively and their application in fuel cells.

Erlebacher et al. investigated the integration and activity of Pt−npAu electrode material in H_2−PEMFC. They employed the chemical reduction of a Pt salt by hydrazine inside the pores of a npAu leaf (~100 nm thick), as described in the previous section (cf. Figure 5 a). Following the membrane electrode assembly approach, the Pt−npAu leaves were sandwiched on both sides of a Nafion membrane, stabilized by either Teflon-treated carbon or stainless steel plates as current collectors. The material thus was employed both as anode (H_2 oxidation) and cathode material (ORR). Some of the results are displayed in Figure 7. The Pt−npAu PEM cells produced up to 240 mW per cm^2 and 4.5 kW per g of Pt. Overall, the performance of the material was assessed to be very promising. However, further studies have to be carried out to test the practicability of the material, especially with respect to handling and stability, that is, degradation of the catalyst over a duration of weeks and months.

Although fuel cells using hydrogen as fuel are very promising in terms of power density and efficiency, until now, the storage and supply of hydrogen has limited their application. Especially the storage of hydrogen has proved to be very demanding in terms of quantity and leaking issues. Fuel cells circumventing these problems use liquids such as methanol or formic acid as fuel. Methanol (also methyl alcohol or wood alcohol) is a main feedstock for the industrial production of several bulk and commodity chemicals and is produced and, thus, available in the range of millions of tons per year.[110] Most importantly, methanol is increasingly generated from green and sustainable resources, such as from landfill and bio gas. Already, in the 1990s, the Nobel prize winner George A. Olah advocated methanol as a proper replacement for fossil fuels, proclaiming the methanol economy.[111]

Cyclovoltammograms for the electro-oxidation of methanol in alkaline solution using Pt−npAu electrodes (and uncoated npAu) are shown in Figure 8. The oxidation of methanol on Au and Pt−Au surfaces proceeds at two potentials with different mechanisms. At lower potentials (0−100 mV vs Ag/AgCl), methanol is oxidized to formate via a four-electron transfer:

$$CH_3OH + 5OH \rightarrow HCOO^- + 4H_2O + 4e^- \quad (3)$$

and at higher potentials (>~ 600 mV vs Ag/AgCl), through a six-electron process to carbonate:

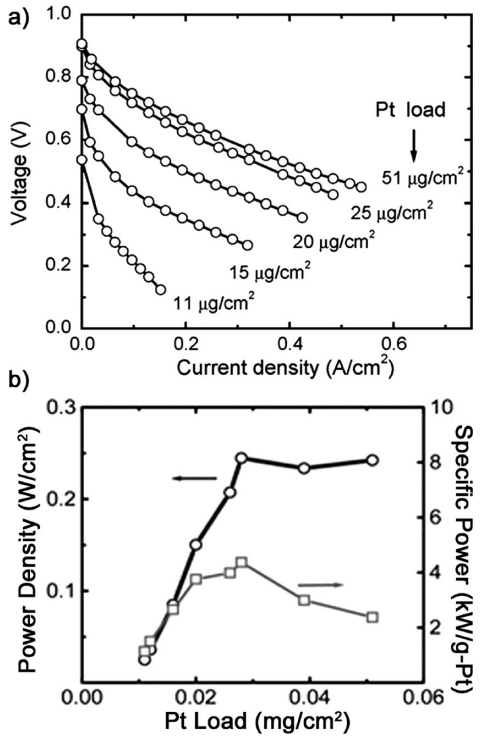

Figure 7. Pt–npAu in a H_2–PEMFC application. (a) Voltage–current polarization curves for different Pt loadings. (b) Maximum power density and specific power of Pt–npAu for various Pt loadings. Obviously, a maximal performance is achieved at loadings of ~25 μg Pt/cm^2 (reproduced from ref 26, copyright Elsevier, 2012).

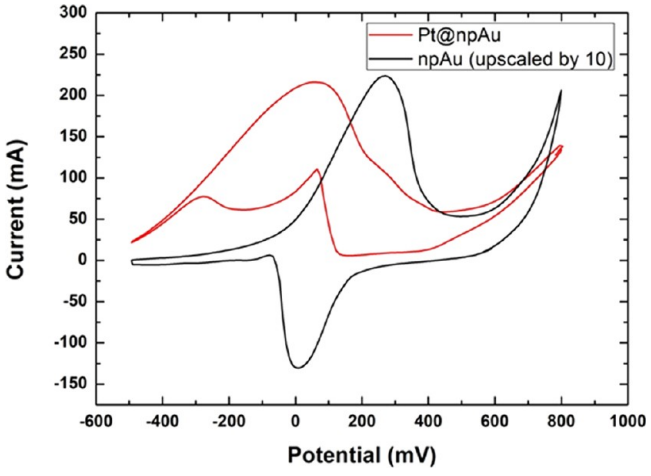

Figure 8. CV curves recorded in 1 M KOH (Riedel-de Haen, p.A.) solution containing 1 M MeOH (VWR, >99.8%). The oxidation signal of the Pt@npAu sample could be increased by 1 order of magnitude in comparison with the uncoated disk. The oxidation peak on the reverse scan is characteristic of a platinum system (regeneration of active metallic Pt surface based on desorption of OH_{ads} or reduction of Pt oxides). See, in contrast, the reduction peak of the pure gold system. (Ag/AgCl reference electrode; scan rate 10 mV/s; npAu disks of 5 mm diameter and 250 μm thickness were used as working electrode).[107].

$$CH_3OH + 8OH^- \rightarrow CO_3^{2-} + 6H_2O + 6e^- \quad (4)$$

The activity for methanol oxidation strongly depends on the chemisorption and activation of OH^- on the electrode surface. The pure npAu electrode lacks activity, especially for the oxidation of methanol at low potential. After adding Pt to the Au surface (cf. procedure shown in Figure 6), however, the current is increased by 1 order of magnitude (Figure 8). The key to this dramatically increased activity is the bifunctional activity involving Au as well as Pt sites on the electrode surface for further oxidation of the carbonyl species (carbonate and formate),[112] as, for example, in the following manner:

$$Pt\text{-}CO_{ads} + Au\text{-}OH_{ads} \rightarrow CO_2 + H^+ + Pt + Au + e^- \quad (5)$$

Problems associated with the use of methanol in fuel cells are related to its high vapor pressure and flammability, as well as with the permeability of the Nafion membrane for methanol, leading to an undesired cross over flux.

Formic acid as an alternative fuel has proved to be advantageous in this respect, allowing for a smaller fuel cell design.[113,114] Industrially, formic acid is derived on the order of millions of tons from the oxidation of methanol and is thus readily available.[115] Because the oxidation state of formic acid is higher than that of methanol, its power density is only 1740 W·h/g, yet for the above-mentioned reasons, one can run formic acid fuel cells with higher concentrations of the fuel (e.g., 70 wt %), compensating the lower power density. In addition, the electrochemical driving force in DFAFCs is higher, theoretically allowing open circuit potentials of about 1.45 V.

According to Behm and co-workers, the oxidation of formic acid on Pt surfaces in an acidic environment generally proceeds via an indirect dehydration pathway (eq 6), a formate pathway, or a direct dehydrogenation process (eq 7):[116]

$$HCOOH \rightarrow CO_{ads} + H_2O \rightarrow CO_2 + 2H^+ + 2e^- \quad (6)$$

$$HCOOH \rightarrow CO_2 + 2H^+ + 2e^- \quad (7)$$

The important difference between these mechanisms is the formation of intermediates, such as CO, which is known to strongly bond and, thus, potentially poison active sites on the Pt surface. At low potentials (i.e., 0.2 V vs RHE), the oxidation of CO on the Pt surface proceeds very slowly, inhibiting the conversion of formic acid at potentials below 0.6 V.[116]

Infrared spectroscopic results on bimetallic Au–Pt surfaces indicate that the mechanism based on the direct dehydrogenation (eq 7) is promoted.[117] Accordingly and similar to the case of the electro-oxidation of methanol, Pt–npAu electrodes can have superior catalytic activity due to a bimetallic synergistic effect.

Wang et al. succeeded recently in the fabrication of a highly active and stable Pt–npAu catalyst employing a sandwich design.[117] First, a layer of Pt was deposited on a npAu electrode (npAu–Pt), and subsequently, different amounts of Au in the form of small islands were deposited on the npAu–Pt electrode (Figure 9). Even very small amounts of Au greatly enhanced the activity of the catalyst for the favorable dehydration of formic acid at low potentials. In addition, the durability of the electrode could be considerably enhanced by combining both metals (Figure 9). This electrode design has three very favorable characteristics: it needs very low Pt loadings, exhibits great tolerance against CO poisoning, and shows superior stability/durability as compared with a Pt/C electrode. On the basis of in situ infrared spectroscopic characterization, Wang et al. concluded that the direct oxidation of formic acid (eq 7) at low potentials indeed greatly benefits from the presence of Au and isolated Pt atoms on the surface.[117]

dx.doi.org/10.1021/cs300231u | ACS Catal. 2012, 2, 2199–2215

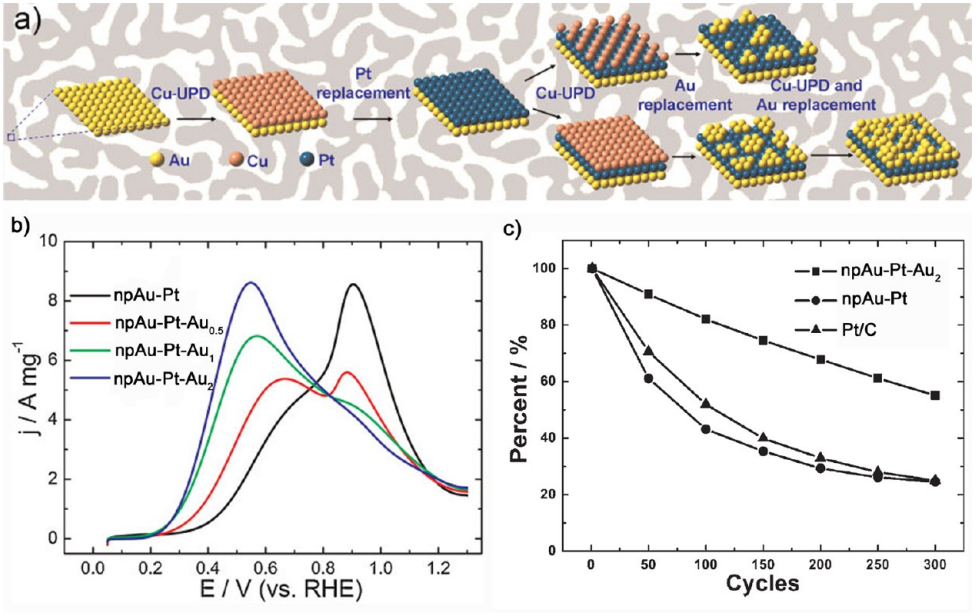

Figure 9. Electro-oxidation of formic acid using Pt–npAu electrodes. (a) Schematic illustration of the fabrication procedure of NPG–Pt_1–Au_x catalysts. (b) Oxidation of formic acid: CV segment of the forward scan of npAu-Pt_1–Au_x catalysts in 0.1 M $HClO_4$ and 0.05 M HCOOH. (c) Loss of activity of npAu-Pt, npAu–Pt-Au, and a commercial Pt/C electrode material after extensive cycling in 0.1 M $HClO_4$ between 0.05 and 1.5 V (reproduced from ref 117, copyright Wiley and Sons, 2012).

3.3. Pt-Modified npAu for Electrocatalytic Sensing.

NpAu electrode materials offer very high surface areas combined with high catalytic activity and durability. As a consequence, they are especially suitable as highly sensitive electrochemical sensors. The working principle of an electrochemical sensor is based on the selective catalytic reaction of a probe molecule. The associated current works as the sensing signal. Several studies during recent years have demonstrated the large potential of npAu electrodes for sensing (detection and quantification) of various important biological substances, such as glucose,[7,14,118,119] dopamine (DA),[10] ascorbic acid (AA),[10] hydrogen peroxide (H_2O_2),[15] and NADH.[13] In the context of this review, we focus on glucose because it is a prime biomolecule and the main source of energy for the human body. Its sensing is of practical importance in the context of medical diagnosis, but also in fermentation and food production processes, for example, in the production of wine.

Common sensors use enzymes as the sensitive "antenna" for glucose detection and the metal electrode as current collector. However, these sensors are prone to fast deactivation and loss of activity as a consequence of the degradation of the enzyme.[120] Novel sensor materials that combine high sensitivity and selectivity in the detection of glucose and appreciable durability are of great interest. Suitable electrode materials typically comprise precious metals, such as Au, Pt, Pd, Ag, and their alloys.[121,122] In this context, Huang et al. studied npAu and Pt-modified npAu electrodes for glucose sensing (Figure 10).[119] The sensing of the electrode material in neutral media is based on the electro-oxidation of glucose to gluconolacetone at potentials between 0.2 and 0.4 V (vs standard calomel electrode (SCE)).[123]

The oxidation of glucose was studied under neutral pH (phosphate buffer saline, pH 7.4) because this mimics physiological conditions, for example, in human blood. The npAu type electrode material showed a more than 100-times-increased current as compared with a smooth Au electrode

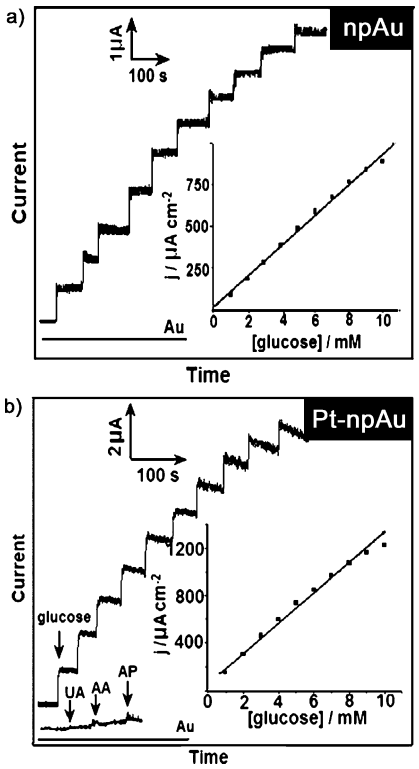

Figure 10. Amperometric detection of glucose using npAu (at +0.35 V) and Pt–npAu (at +0.2 V) electrodes. The current vs time curves were recorded while successively adding 1 mM glucose, as well as 0.02 mM uranic acid (UA), 0.1 mM ascorbic acid (AA), 0.1 mM adenosine phosphate (AP). The electrolyte was phosphate buffered saline, pH 7.4, containing 0.1 M KCl, hence, mimicking physiological conditions. The insets show the corresponding calibration curves for glucose quantification (reproduced from ref 119, copyright Elsevier, 2012).

owing to its roughness and high surface area. As in the case of methanol or formic acid oxidation, the activity could be

dx.doi.org/10.1021/cs300231u | ACS Catal. 2012, 2, 2199–2215

increased by adding small amounts of Pt onto the Au surface. If the Pt coverage did not exceed 60%, the Pt−npAu electrode showed an increased activity by ∼24%. At higher coverage, the Pt formed 3-dimensional islands on the surface, which apparently were less active for the electro-oxidation. It is noteworthy that under alkaline conditions, Pt addition was not beneficial for catalytic activity. The higher activity of the Pt−npAu electrode materials was attributed to a synergistic effect on the oxidation of glucose.[124,125] Aside from the high activity and selectivity of the npAu electrode material, its stability was the focus of the study by Huang et al. They investigated the CV response during the oxidation of glucose over a period of 1 month (testing every 5 days). The electrode material retained 95% of its initial activity after this period, indicating a very high stability.

4. COMBINING NANOPOROUS GOLD WITH ORGANIC CATALYTIC ENTITIES

A further option of adding a specific functionality to the npAu material is its functionalization by organic catalytic entities, generating specific reactivity. Molecules or complexes are chemically immobilized on the npAu substrate so that homogeneous catalysts that are otherwise dispersed in a reaction medium can be turned into a heterogeneous catalyst accompanied by the advantages of better recyclability, easy separation of the catalyst from the products and reaction media, or electric conductivity for electrocatalytic applications and sensors.

The potential of npAu for this kind of building block design was demonstrated in several publications during the last ∼5 years. Shulga et al. and Qiu et al. demonstrated that npAu is a good carrier for catalysts and biomolecules, such as proteins and enzymes.[126−130] The cornerstone for the immobilization of the molecules is the interaction and bonding of sulfur- and nitrogen-containing moieties of the biomolecule with the Au surface.[130] The comparably large pore size of the npAu structure, in the range of 30 nm, still allows proteins to take their preferred orientation and conformation, respectively, after immobilization. This is of critical importance with respect to their activity. For example, Qiu at al. employed enzyme-functionalized npAu for the detection of ethanol and glucose by immobilization of alcohol dehydrogenase and glucose oxidase, respectively.[13] Zhu et al. combined a npAu electrode with cytochrome *c* when preparing a H_2O_2 sensor working in physiological media.[11] A further very interesting combination is the immobilization of antibodies on the npAu surface as label-free electrochemical immunosensors. Wei et al. demonstrated that an ultrasensitive npAu-based immunosensor for the detection of cancer biomarker prostate-specific antigen can be prepared by immobilization of an anti-PSA antibody onto the npAu surface.[131] The electrocatalytic oxidation and reduction of $K_3Fe(CN)_6$ at the electrode surface could be used as a sensitive reaction toward the formation of the antigen and the specific antibody with very high sensitivity, as low as 3 pg/mL of antibody.

In the following, we first report on exemplary chemical means of bonding organic molecules onto the npAu surface. Second, we describe results using functionalized npAu electrodes as sensitive redox electrodes. In the last section, we describe applications of enzyme-modified npAu electrodes in more detail.

4.1. Two-Step Immobilization of Organic Entities Using Click Chemistry. For a stable and reproducible immobilization of an organic molecule onto the npAu surface, a chemical bond between the organic molecule and the gold surface is necessary. Although gold lacks reactivity toward many chemical reactions,[51] it exhibits a very selective reactivity toward bond formation with some heteroatoms, such as sulfur, nitrogen, and chlorine.[39,132] This specific reactivity of Au (for example, for the bonding of sulfur) was used extensively for the preparation of self-assembled monolayers onto Au substrates.[133,134] It is thus obvious to employ this kind of chemistry also for the immobilization of catalytically active molecules onto the npAu surface. To prevent direct reaction of the catalytically active moiety with the Au surface, a two-step approach is most suitable, comprising first the attachment of a layer of linker and spacer molecules and, in a second step, the chemical bonding of the catalytic active molecule to the linker molecules (cf. Figure 11).

The deposition of the first layer of linker molecules works in analogy to the self-assembly of thiol molecules on Au surfaces. In the second step, a so-called "click reaction" can be employed. In 2001, Sharpless and co-workers coined this term for their Cu(I)-catalyzed Huisgen 1,3-diploar cycloaddition of azides and terminal alkynes, forming 1,2,3-triazoles (cf. Figure 11).[135] The resulting triazole rings are chemically exceptionally inert to reactive conditions (e.g., hydrolysis and oxidation). Because the click reaction can be used at a wide range of temperatures, pH values, and solvents, it is a very suitable and versatile chemical tool for attaching organic entities.

4.2. Highly Sensitive Redox Electrodes. Following the above-described two-step approach for the organic functionalization of npAu, redox-active ferrocene entities can be attached to the npAu surface (Figure 11). For the immobilization of the linker and a diluting thiol (ensuring a sufficient distance between the linker and, thus, the later attached functionalities on the surface), the nanoporous gold substrate was immersed in a solution containing 50 mM 11-azidoundecane-1-thiol and 150 mM octane-1-thiol (Sigma Aldrich, >98.5%) in ethanol for 3 days (Figure 11b). The subsequent attachment of the electroactive species propynoyl ferrocene was achieved by immersing the npAu disk in a solution containing 0.25 M propynoyl ferrocene, 0.1 M Cu[TBTA]PF_6, and 0.25 M hydroquinone (Sigma Aldrich, >99.0%) in DMSO (Merck, p.A.)/H_2O 3:1 for 24 h. To compare current densities between npAu and a planar system, a gold foil was treated precisely the same way (Figure 11c).

Using this two-step approach provides good control over the formation of the self-assembled monolayer and also avoids a potential direct reaction of a ferrocene group with the Au surface. The resulting ferrocene/npAu system was characterized using cyclic voltammetry (Figure 11c). Due to its high surface area, the resulting current density (referenced to the geometric surface of the sample) was nearly 2 orders of magnitude larger than that of a planar Au electrode.

4.3. Enzyme-Modified Sensors. Biomolecules such as enzymes are biological catalysts. Humans as well as every other living organism on earth rely on these molecules for selectively catalyzing chemical reactions in our body. In terms of selectivity, enzymes are the role model of a catalyst. The combination of enzymes as the catalytically active "antenna" and the npAu as high-surface-area, biocompatible, and conductive substrate is thus very promising.

Qiu et al. developed a biocatalytic sensor based on the combination of npAu and enzymes for the detection of alcohols, such as ethanol, and glucose.[13] They prepared a

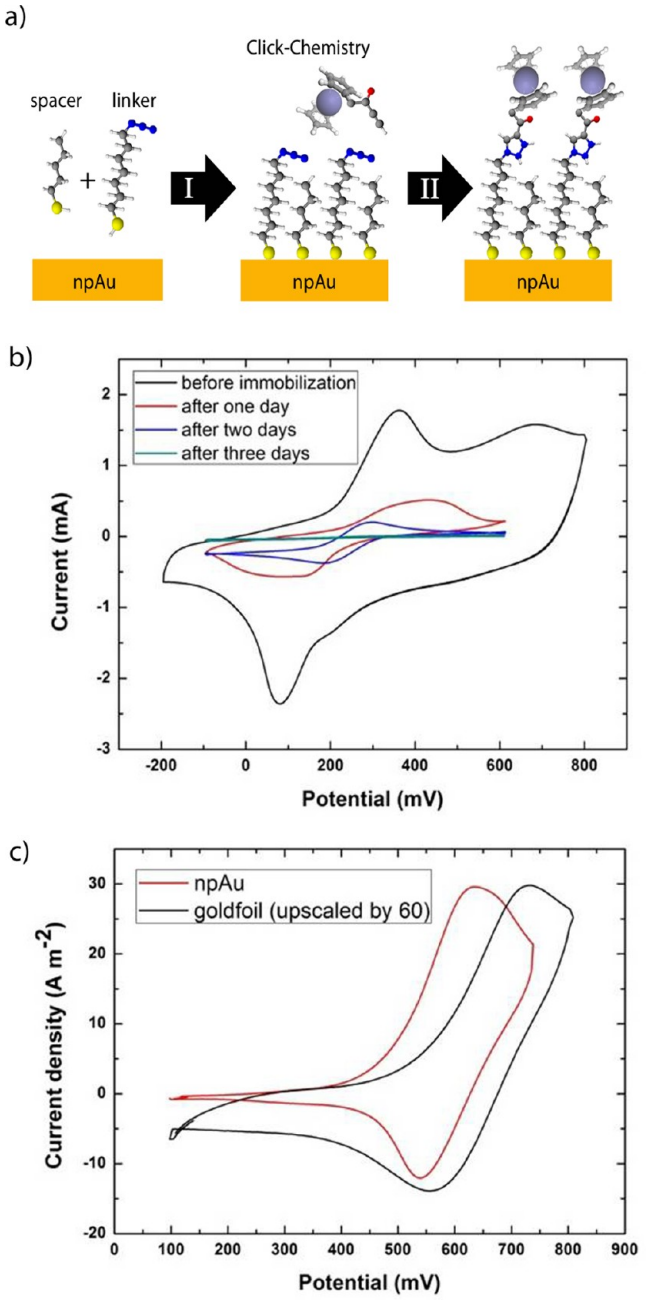

Figure 11. (a) Immobilization of a catalytically active functionality onto the npAu substrate. First, a monolayer of thiols working as a "linker" is deposited by self-assembly. In the second step, the desired functionality (here, ferrocene) is bonded to the first linker by click chemistry. (b) Cyclovoltammograms (CV) after linker immobilization (step I). The CVs were measured in 0.1 M KCl (Acros, p.A.) with 5 mM $K_3Fe(CN)_6$ (Merck, p.A.) vs Ag/AgCl and at a scan rate of 10 mV/s. The redox reaction of ferrocene on the npAu surface was used to monitor the degree of coverage of the Au surface by the linker. The absence of any current after 3 days indicates that the entire surface is covered by the linker molecules. (c) Cyclic voltammogram of propynoyl ferrocene clicked to the linker adsorbed on the nanoporous gold and a planar gold foil substrate (step II). The current density of the npAu electrode is higher than for the planar electrode by a factor of 60. The CVs were measured in 0.1 M $HClO_4$ (Sigma Aldrich, ACS reagent 70%) vs a Ag/AgCl electrode with a scan rate of 10 mV/s.[107]

nanoporous gold electrode from Au–Ag alloy leaf attached to a polished glassy carbon electrode (GCE) working as backbone. For detection of the alcohols, the npAu–GCE electrodes were coated with glucose oxidase (GOD) and alcohol dehydrogenase (ADH), respectively. To prevent fast degradation and leakage of the enzymes, the npAu/enzyme electrodes were bedewed with a cation exchange polymer (Nafion). The Nafion/ADH–npAu/GCE catalyst showed a linear response in the amperometric current–time curve over the ethanol concentration range of 1–8 mM with a sensitivity of 0.19 mA mM^{-1} and a detection limit of 120 mM of ethanol. In a similar fashion, the Nafion/GOD–npAu/GCE responded linearly to a glucose concentration in the range of 1–18 mM with a sensitivity of 0.049 A mM^{-1} and a detection limit of 196 mM of glucose. Particularly important is the good stability of the npAu/enzyme electrode sensors; the authors detected a loss of activity of as little as 5% over the duration of 1 month.

Another enzyme-modified sensor in combination with npAu in the form of an encapsulated cytochrome *c* (cyt-*c*) npAu electrode for H_2O_2 sensing[136] was developed by Zhu et al. Different from that described in the previous section about the preparation of npAu, in this contribution, the authors used a different procedure for generation of the nanoporous gold electrode. As the starting material, Zhu et al. prepared an assembly of Au and Ag nanoparticles using a linker molecule (1,5-pentanedithiol). In the next step, the Ag was leached out of this Au–Ag particle assembly by galvanic replacement of Ag atoms by Au from a $HAuCl_4$ solution at room temperature. Because one Au^{3+} ion leaches three Ag atoms, the resulting structure consists of a nanoporous and rough gold surface. After preparation of the npAu electrode, it was coated with a solution of the enzyme (cyt-*c*) and dried. The integrity of the enzyme after immobilization was monitored by UV/vis spectroscopy. The major absorption wavelength of cyt-*c* adsorbed on the npAu electrode was only slightly red-shifted (from 409 to 411 nm), indicating that no denaturation of the enzyme occurred during immobilization and the conformation of the immobilized enzyme was still intact. This finding also reconfirms the good biocompatibility of the npAu material. The cyt-*c*-encapsulated npAu bioelectrode responded linearly to a H_2O_2 concentration range of 10 μM to 12 mM, with a detection limit as low as 6.3 μM. Noteworthy, this biosensor showed not only good biocompatibility but also convincing stability: over a duration of 1 month, almost no degradation was detected.

5. COMBINING NANOPOROUS GOLD WITH METAL OXIDES

A further very promising approach for tuning the catalytic performance of npAu is its combination with metal oxides. As in the case of Au nanoparticles on metal oxide supports, the interface between both partners is expected to evoke high catalytic activity. The principles of an "inverse" gold catalyst were first investigated by Rodriguez and others under UHV conditions, employing metal oxide particles on flat gold single-crystal surfaces.[137] Nanoporous gold as a high-surface-area gold support is ideally suited to transfer these principles of Au-supported metal oxide particles to a catalytic system working under ambient pressure conditions. The objective here is two-fold: by reversing the classical order of Au particles dispersed on a metal oxide support, on one hand, mechanistic insights can be gained because the interface between both partners is conserved while the roles of the support and the one of the particles are reversed. On the other hand—and more importantly from an applied point of view—one of the obstacles for commercial application of Au-based catalysts,

dx.doi.org/10.1021/cs300231u | *ACS Catal.* 2012, 2, 2199–2215

resulting from the inherent instability of Au nanostructures at elevated temperatures, can be tackled. This drawback is a consequence of the low melting point of Au, which is only 1063 °C, as compared, for example, with Pt, which has a melting point of 1770 °C. Since oxides, such as titania (1843 °C), have inherently higher melting points, the reversed order—oxide nanoparticles supported on an Au substrate—can be expected to be much more stable against coalescence. Indeed, recent studies on metal oxide-modified nanoporous gold not only proved this principle but also revealed that the oxide deposits stabilize the nanoporous gold structure.[27,28] For example, although unmodified npAu starts coarsening at temperatures of ~200 °C, no change in the ligament diameter (~30 nm) was observed up to 1000 °C after deposition of Al_2O_3.[138]

In the following, we will discuss two different and exemplary approaches for coating the inner surface of npAu: first, a deposition process from the gas phase (CVD and ALD) and, second, an experimentally less demanding approach using a liquid precursor.

5.1. Gas Phase Deposition: CVD-Modified Nanoporous Gold. Chemical vapor—more specifically, atomic layer—deposition (ALD) was shown to be an especially dedicated gas phase deposition technique for the coating of high-aspect-ratio materials.[97,139] Already in the case of free-standing films of npAu with a thickness of 200−300 μm and pore sizes of about 30 nm, the aspect ratio of the pores amounts to several thousands. The slow diffusion of molecules into inner sections of the material is a major obstacle when aiming at homogeneous coating of the inner surface and avoiding clogging of pores close to the outer surface. ALD consists of self-limited surface reactions (i.e., chemisorption) of precursors (cf. Figure 12). This limitation makes ALD an ideally suited technique for such high-aspect-ratio materials.

Recently, Biener et al. reported on the atomic layer deposition of Al_2O_3 and TiO_2 on the interior surface of npAu, generating subnanometer-thick and homogeneous coatings.[138] In addition to the impact of the coating on the mechanical properties of the material, they also investigated the catalytic properties of the composite material. In this context, Biener et al. particularly emphasized titania-coated npAu because titania is, of course, known to lead to highly active gold catalysts. Titania was coated on the interior surface by subsequently dosing water and $TiCl_4$ in a warm wall reactor at 100 °C. $TiCl_4$ strongly reacts with water, forming TiO_2 and HCl, which desorbs from the surface so that it is purged out of the system. Interestingly, although the interaction of water or hydroxyl with the Au surface is generally very weak,[140] the concentration of these species on the surface is apparently sufficient to generate even closed layers of titania, a fact that is most likely a consequence of the high concentration of water in air, resulting in a condensed layer of water before the sample is introduced into the ALD system. The resulting growth rate of TiO_2 was determined to be ~0.07 nm per ALD cycle. Because the lattice spacing for a O−Ti−O unit of the (101) plane of anatase TiO_2 is ~0.35 nm,[141] this growth rate corresponds to about 1/5 of a monolayer coating per ALD cycle.

The aerobic oxidation of CO was investigated as an exemplary reaction to assess the catalytic activity of the TiO_2−npAu composite material (Figure 12).[138] Samples that initially had a closed layer of titania did not show any catalytic activity for the CO oxidation. This is not unexpected, since titania itself is not an active catalyst for aerobic CO oxidation at these temperatures, and closed layers of thick titania films

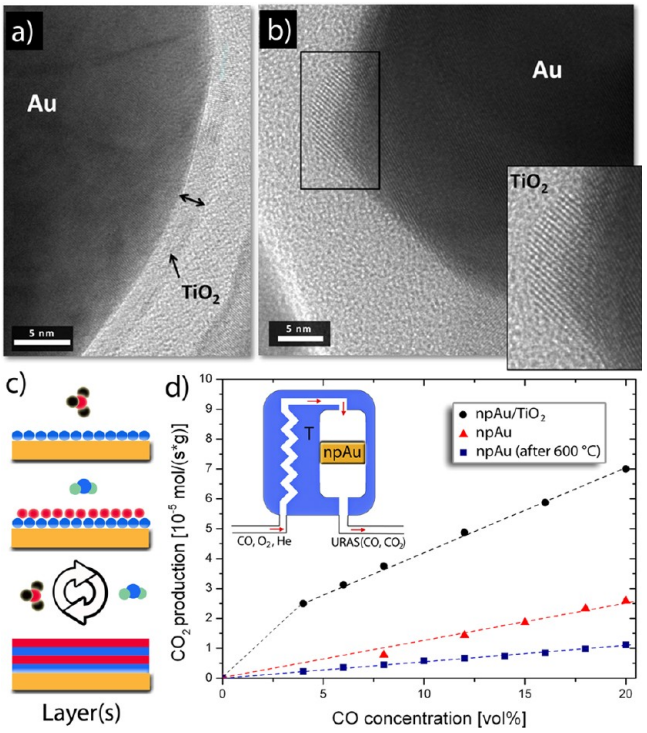

Figure 12. TiO_2 decorated npAu: (a, b) TEM images after heating an ALD-coated sample (30 cycles) to 600 °C. The initially closed layer of titania (a) breaks up, resulting in titania nanoparticles (b) on the gold surface (scale bars are 5 nm). (c) Schematic drawing showing the steps of an ALD. (d) Aerobic oxidation of CO at 60 °C using npAu and titania-modified npAu (10 cycles) in a continuous flow reactor. (Results for bare npAu sample annealed to 600 °C without titania doping is displayed for comparison; 30 vol % O_2; helium as carrier gas; total flow of gases, 50 mL/min).[138] (TEM, image courtesy of K. Frank and A. Rosenauer, University Bremen; section d is reproduced from ref [138], copyright American Chemical Society, 2012).

obviously passivate the surface.[142] However, after annealing the sample at temperatures of ~550 °C prior to catalytic measurements, activity was detected. TEM and Raman spectroscopy revealed that at these elevated temperatures, the as-prepared amorphous layer of TiO_2 fractures and breaks up into titania crystallized (anatase) metal oxide nanoparticles ~5 nm in size.[138,143] As a result, titania as well as Au surface sites are exposed to the reactants (Figure 12).

The composite material showed an amplified activity for the oxidation of CO by a factor of ~5 (measured at 60 °C; cf. Figure 12).[37] Recent work from Yates et al. suggests that the interface between gold and titania plays a key role in the catalytic activity of these systems. Here, the molecular oxygen can be efficiently activated, and CO adsorbed either on Au or on titania sites can react with oxygen located at the interface.[80] The fact that metal oxide nanoparticles on a high-surface-area gold support lead to a strongly increased activity underlines that the interface and a related synergistic effect are important key factors for high catalytic activity of gold-based catalysts.

5.2. Liquid Phase Deposition. In some cases, deposition of a precursor material or the direct deposition of the metal oxide from the *liquid* phase is preferable, since the precursor does not have a vapor pressure high enough to reach appreciable concentrations in the gas phase or simply because of less demanding (and less costly) experimental conditions, allowing, for example, "simple" bench-top chemistry. Here, the

dx.doi.org/10.1021/cs300231u | ACS Catal. 2012, 2, 2199−2215

sample is submersed into the corresponding solution and thus impregnated.

In a first study of this kind, Ding et al. immersed npAu membranes into an ethanol suspension of TiO_2 nanoparticles, depositing TiO_2 particles directly from solution.[29] Yet, this deposition technique resulted in a superficial coating, and most of the particles were found on the outer surface of the material. Nevertheless, the composite material, only 100 nm thick, showed great performance for photocatalytic oxidation of methanol. In a very similar fashion, Wittstock et al. prepared TiO_2–npAu free-standing membranes for the gas phase oxidation of CO.[87] Also in this case, the majority of particles were dispersed onto the outer surface of the porous membrane. Nonetheless, the catalytic performance of the material was noticeably improved. The activity of the composite material was enhanced by a factor of ~5 when compared with pure npAu.

Because the direct deposition of existing TiO_2 nanoparticles from suspensions, although comparatively easy, results mostly in an inhomogeneous coating, an alternative route to TiO_2/npAu composites is desirable. Such a route is the impregnation of the material with a suitable liquid precursor, such as titanium isopropoxide (TTIP) and a subsequent reaction forming the metal oxide (e.g., hydrolysis in air). This technique is obviously very similar to the chemical vapor deposition from the gas phase, which offers a broad variety of possible precursor components. After submersing npAu in TTIP and hydrolysis in air, calcination at 400 °C in helium leads to finely dispersed coatings of TiO_2 across the whole cross section of a 300 μm npAu membrane.[143]

In line with previous experiments on the catalytic oxidation of CO, the activity of the composite material was enhanced as compared with the pure npAu sample (Figure 13). In addition to the amplified activity, the composite material also showed improved resistivity to temperature-induced coarsening. Although the gold ligaments in pure npAu start to coarsen at temperatures of ~200 °C, no structural changes in the composite material were observed, even after heating to temperatuers above 400 °C. This increased structural stability also indicates stable catalytic activity at elevated temperatures. For example, at 250 °C, the activity for CO oxidation was nearly constant, even under continuous operation for many days. After 72 h, the catalyst lost only ~4% of its initial activity.

In another example, coatings of praseodymia were realized by immersing npAu membranes into $Pr(NO_3)_2$ solutions and subsequent hydrolysis and calcination at 500 °C.[87,143] This rather uncommon metal oxide is right next to cerium in the periodic table of the elements, which is known to result in highly active gold catalysts, yet the oxygen mobility in the case of praseodymium oxide is even higher than that of ceria, and indeed, the praseodymia-npAu composite material showed strongly improved catalytic activity, too (Figure 13). This finding underlines the versatility of the approach and opens up a deliberate material design using different metal oxides with specific characteristics.

In summary, composite materials of npAu and certain metal oxides are highly active and stable catalysts. They combine high activity at low temperatures, not attainable by other precious metal-based catalysts, such as Pt, with a superior catalyst durability and stability at temperatures of several hundred degrees. This enables novel applications of gold-based catalysts, such as in the automotive converter. In addition, this type of inverse catalyst is a valuable tool for addressing and investigating the interaction between the precious metal and the oxide.[137−145] Accordingly, a more detailed investigation of the systems may also contribute to the mechanistic understanding of Au-based catalytic systems in general.

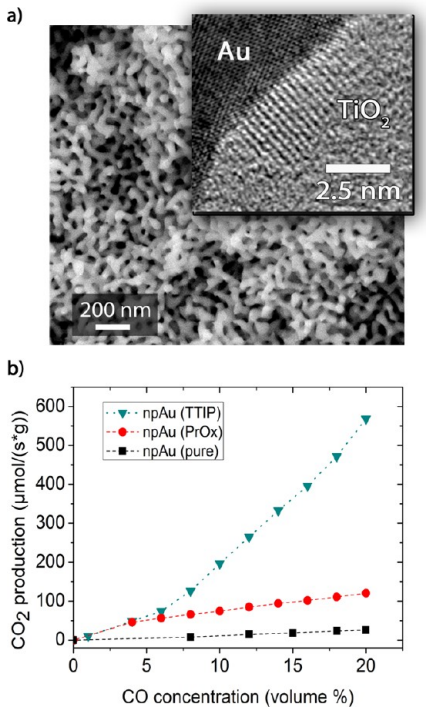

Figure 13. Oxide-modified npAu. (a) Cross-sectional SEM of a titania-coated npAu membrane. The sample was first submersed in a TTIP precursor containing solution and subsequently calcined at 500 °C in air. The inset shows a high resolution TEM of a TiO_2 particle on the npAu surface. (b) Catalytic conversion of CO using pure npAu and oxide-modified npAu at 60 °C (30 vol % O_2 and total flow rate of 50 mL/min).

6. SUMMARY AND FUTURE OUTLOOK

In this review, we reported and discussed various possibilities of deliberately modifying the surface of npAu and its chemistry by introducing metals, metal oxides, and molecular catalysts into the porous structure, leading to high-performance catalysts for heterogeneous catalysis, electrocatalysis, and electrocatalytic sensing. NpAu is generated by electrochemical means, which is the corrosion of a Au alloy containing at least one less-noble constituent, such as silver. The particular advantage of this approach is a broad flexibility with respect to sample dimensions and comparatively simple preparation by chemical benchtop techniques. Sample dimensions from about 100-nm-thick films all the way up to centimeter-sized cubes can be generated by simply submersing the corresponding alloy in nitric acid. The resulting mesoporous gold can be employed as a very selective and active catalyst for aerobic oxidation reactions in liquid as well as gas phase catalysis. However, this electrically conductive and high surface area material also offers a broad range of opportunities for tuning the surface with additives. In the context of electrocatalysis, the addition of small amounts of Pt proved to increase the activity of the material. The electrocatalytic reaction of molecules on the catalysts surface can be used not only for energy harvesting, such as in fuel cell applications, but also for sensing. For example, the current generated by the oxidation of glucose on the npAu electrode surface can be used for quantification and detection of

this very important biomolecule. By adding Pt onto the npAu surface, the current response and, thus, the sensitivity of this sensor can be considerably increased.

In a comparable way, molecular catalysts such as enzymes or metal complexes can be immobilized and bonded onto the electrically conductive npAu electrode surface. In this way, not only can the high activity and selectivity of homogeneous catalysts be implemented into a heterogeneous catalyst but also the current stemming from electrochemical oxidation reactions can be used for detection and quantification of probe molecules. For example, biomolecules such as alcohol dehydrogenase and glucose oxidase can be immobilized onto the npAu structure, taking advantage of their selectivity with respect to the oxidation of alcohols, such as ethanol, and glucose.

With respect to heterogeneous gas phase catalysis, the addition of metal oxides (TiO_2, CeO_2, Fe_2O_3, etc.) onto the npAu surface is a very promising route for the generation of highly active and durable catalysts. In analogy to gold nanoparticles, which typically have to be deposited on a metal oxide support to show activity for aerobic oxidation reactions, the addition of a metal oxide onto the npAu resulted in a considerably increased activity for the aerobic oxidation of CO. In addition to the amplified activity, the oxide-modified catalyst showed unprecedented stability at temperatures of several hundred degrees Celsius, likely owing to a suppression of surface self-diffusion of gold atoms and, thus, coarsening of the nanostructures by the metal oxide.

Although humans used this type of nanoporous gold material for centuries in artwork, its technological applications as, for example, in catalysis are very young and have evolved during the last 10 years. For example, the finding that pure npAu is a very active catalyst for aerobic oxidation reactions dates back only about 6 year. Within these last years, the efforts of several research groups around the world have been drawn to this subject, and the applications of this material in many catalytic arenas have been investigated. From an applied and economic point of view, further efforts will be necessary to bring nanoporous gold into industrial applications. For example, the material investment (namely, the use of a bulk gold material) appears to be an impediment; however, the large flexibility of the material dimensions allows for an intelligent and indeed economically viable application of the material, for example, in the form of thin films or hierarchical structures. From a scientific point of view, further investigation and understanding of the catalytic processes on the atomic level will be of great importance. First attempts have already proven that the extended gold surface is particularly suited to transfer insights obtained from model studies on Au single crystal surfaces to the catalytic behavior of npAu under ambient and so-called "real-world" catalytic conditions, thus paving the way to a predictable catalyst.

AUTHOR INFORMATION

Corresponding Author

*E-mail: wittstock1@llnl.gov (A.W.), mbaeumer@uni-bremen.de (M.B).

Notes

The authors declare no competing financial interest.

ACKNOWLEDGMENTS

The authors thank University Bremen and the state of Bremen for financial support. A.W.'s work was performed under the auspices of the U.S. Department of Energy by LLNL under Contract DE-AC52-07NA27344.

REFERENCES

(1) Wittstock, A.; Biener, J.; Erlebacher, J.; Bäumer, M. *Nanoporous Gold: from an Ancient Technology to a Novel Material*; 1st ed.; Royal Society of Chemistry: London, 2012; Vol. *1*; p 250.
(2) Covert, L. W.; Adkins, H. *J. Am. Chem. Soc.* **1932**, *54*, 4116−4117.
(3) Smith, A. J.; Trimm, D. L. In *Annual Review of Materials Research*, Annual Reviews: Palo Alto, 2005; Vol. *35*, pp 127−142.
(4) Ivanov, E.; Grigorieva, T.; Golubkova, G.; Boldyrev, V.; Fasman, A. B.; Mikhailenko, S. D.; Kalinina, O. T. *Mater. Lett.* **1988**, *7*, 51−54.
(5) Wittstock, A.; Zielasek, V.; Biener, J.; Friend, C. M.; Bäumer, M. *Science* **2010**, *327*, 319−322.
(6) Biener, J.; Wittstock, A.; Zepeda-Ruiz, L. A.; Biener, M. M.; Zielasek, V.; Kramer, D.; Viswanath, R. N.; Weissmuller, J.; Bäumer, M.; Hamza, A. V. *Nat. Mater.* **2009**, *8*, 47−51.
(7) Ding, Y.; Chen, M. W. *MRS Bull.* **2009**, *34*, 569−576.
(8) Erlebacher, J.; Seshadri, R. *MRS Bull.* **2009**, *34*, 561−568.
(9) Seker, E.; Reed, M.; Begley, M. *Materials* **2009**, *2*, 2188−2215.
(10) Qiu, H.-J.; Zhou, G.-P.; Ji, G.-L.; Zhang, Y.; Huang, X.-R.; Ding, Y. *Colloids Surf., B* **2009**, *69*, 105−108.
(11) Qiu, H.; Xue, L.; Ji, G.; Zhou, G.; Huang, X.; Qu, Y.; Gao, P. *Biosens. Bioelectron.* **2009**, *24*, 3014−3018.
(12) Zhu, A.; Tian, Y.; Liu, H.; Luo, Y. *Biomaterials* **2009**, *30*, 3183−3188.
(13) Qiu, H. J.; Xue, L. Y.; Ji, G. L.; Zhou, G. P.; Huang, X. R.; Qu, Y. B.; Gao, P. J. *Biosens. Bioelectron.* **2009**, *24*, 3014−3018.
(14) Yin, H. M.; Zhou, C. Q.; Xu, C. X.; Liu, P. P.; Xu, X. H.; Ding, Y. *J. Phys. Chem. C* **2008**, *112*, 9673−9678.
(15) Zeis, R.; Lei, T.; Sieradzki, K.; Snyder, J.; Erlebacher, J. *J. Catal.* **2008**, *253*, 132−138.
(16) Qian, L. H.; Chen, M. W. *Appl. Phys. Lett.* **2007**, *91*, 083105-1 − 083105-3.
(17) Cattarin, S.; Kramer, D.; Lui, A.; Musiani, M. M. *J. Phys. Chem. C* **2007**, *111*, 12643−12649.
(18) Forty, A. J. *Nature* **1979**, *282*, 597−598.
(19) Forty, A. J.; Durkin, P. *Philos. Mag. A* **1980**, *42*, 295−318.
(20) Pickering, H. W.; Swann, P. R. *Corrosion* **1963**, *19*, 373t.
(21) ISIWeb of Knowledge as of June/2011, Keyword "nanoporous gold".
(22) Biener, J.; Nyce, G. W.; Hodge, A. M.; Biener, M. M.; Hamza, A. V.; Maier, S. A. *Adv. Mater.* **2008**, *20*, 1211−1217.
(23) Hodge, A. M.; Biener, J.; Hayes, J. R.; Bythrow, P. M.; Volkert, C. A.; Hamza, A. V. *Acta Mater.* **2007**, *55*, 1343−1349.
(24) Biener, J.; Hodge, A. M.; Hayes, J. R.; Volkert, C. A.; Zepeda-Ruiz, L. A.; Hamza, A. V.; Abraham, F. F. *Nano Lett.* **2006**, *6*, 2379−2382.
(25) Nyce, G. W.; Hayes, J. R.; Hamza, A. V.; Satcher, J. H. *Chem. Mater.* **2007**, *19*, 344−346.
(26) Zeis, R.; Mathur, A.; Fritz, G.; Lee, J.; Erlebacher, J. *J. Power Sources* **2007**, *165*, 65−72.
(27) Biener, M. M.; Biener, J.; Wichmann, A.; Wittstock, A.; Baumann, T. F.; Bäumer, M.; Hamza, A. V. *Nano Lett.* **2011**, *11*, 3085−3090.
(28) Wittstock, A.; Wichmann, A.; Biener, J.; Bäumer, M. *Faraday Discuss.* **2011**, *152*, 87−98.
(29) Jia, C. C.; Yin, H. M.; Ma, H. Y.; Wang, R. Y.; Ge, X. B.; Zhou, A. Q.; Xu, X. H.; Ding, Y. *J. Phys. Chem. C* **2009**, *113*, 16138−16143.
(30) Liu, X. Y.; Madix, R. J.; Friend, C. M. *Chem. Soc. Rev.* **2008**, *37*, 2243−2261.
(31) Meyer, R.; Lemire, C.; Shaikhutdinov, S. K.; Freund, H. *Gold Bull.* **2004**, *37*, 72−124.

(32) Wittstock, A.; Biener, J.; Bäumer, M. *Phys. Chem. Chem. Phys.* **2010**, *12*, 12919−12930.
(33) Renner, H.; Schlamp, G.; Hollmann, D.; Lüschow, H. M.; Tews, P.; Rothaut, J.; Dermann, K.; Knödler, A.; Hecht, C.; Schlott, M.; Drieselmann, R.; Peter, C.; Schiele, R. In *Ullmann's Encyclopedia of Industrial Chemistry*; Wiley-VCH: Weinheim, 2000.
(34) Frimmel, H. E. *Science* **2002**, *297*, 1815−1817.
(35) Willbold, M.; Elliott, T.; Moorbath, S. *Nature* **2011**, *477*, 195−198.
(36) The World Council of Gold; *About Gold*; http://www.gold.org/about_gold/.
(37) Moskaleva, L. V.; Rohe, S.; Wittstock, A.; Zielasek, V.; Kluner, T.; Neyman, K. M.; Bäumer, M. *Phys. Chem. Chem. Phys.* **2011**, *13*, 4529−4539.
(38) Biener, J.; Biener, M. M.; Nowitzki, T.; Hamza, A. V.; Friend, C. M.; Zielasek, V.; Bäumer, M. *ChemPhysChem* **2006**, *7*, 1906−1908.
(39) Min, B. K.; Alemozafar, A. R.; Biener, M. M.; Biener, J.; Friend, C. M. *Top. Catal.* **2005**, *36*, 77−90.
(40) Haiss, W. *Rep. Prog. Phys.* **2001**, *64*, 591−648.
(41) Weissmuller, J.; Viswanath, R. N.; Kramer, D.; Zimmer, P.; Wurschum, R.; Gleiter, H. *Science* **2003**, *300*, 312−315.
(42) Kramer, D.; Viswanath, R. N.; Weissmuller, J. *Nano Lett.* **2004**, *4*, 793−796.
(43) Jin, H. J.; Kurmanaeva, L.; Schmauch, J.; Rosner, H.; Ivanisenko, Y.; Weissmuller, J. *Acta Mater.* **2009**, *57*, 2665−2672.
(44) Besenbacher, ; , F.; Norskov , J. K. *Prog. Surf. Sci.* **1993** , *44*, 5−66.
(45) Norskov, J. K.; Bligaard, T.; Logadottir, A.; Bahn, S.; Hansen, L. B.; Bollinger, M.; Bengaard, H.; Hammer, B.; Sljivancanin, Z.; Mavrikakis, M.; Xu, Y.; Dahl, S.; Jacobsen, C. J. H. *J. Catal.* **2002**, *209*, 275−278.
(46) Hvolbaek, B.; Janssens, T. V. W.; Clausen, B. S.; Christensen, C. H.; Norskov, J. K. *Nano Today* **2007**, *2*, 14−18.
(47) Janssens, T. V. W.; Clausen, B. S.; Hvolbaek, B.; Falsig, H; Christensen, C. H.; Bligaard, T.; Norskov, J. K. *Top. Catal.* **2007**, *44*, 15−26.
(48) Norskov, J. K.; Bligaard, T.; Hvolbaek, B.; Abild-Pedersen, F.; Chorkendorff, I.; Christensen, C. H. *Chem. Soc. Rev.* **2008**, *37*, 2163−2171.
(49) Christensen, C. H.; Norskov, J. K. *J. Chem. Phys.* **2008**, *128*, 8.
(50) Norskov, J. K.; Bligaard, T.; Rossmeisl, J.; Christensen, C. H. *Nat. Chem.* **2009**, *1*, 37−46.
(51) Hammer, B.; Norskov, J. K. *Nature* **1995**, *376*, 238−240.
(52) Newman, R. C.; Corcoran, S. G.; Erlebacher, J.; Aziz, M. J.; Sieradzki, K. *MRS Bull.* **1999**, *24*, 24−28.
(53) Kameoka, S.; Tsai, A. P. *Catal. Lett.* **2008**, *121*, 337−341.
(54) Kameoka, S.; Tsai, A. P. *Catal. Today* **2008**, *132*, 88−92.
(55) Rouya, E.; Reed, M. L.; Kelly, R. G.; Bart-Smith, H.; Begley, M.; Zangari, G. *ECS Trans.* **2007**, *6*, 41−50.
(56) Wang, X. G.; Qi, Z.; Zhao, C. C.; Wang, W. M.; Zhang, Z. H. *J. Phys. Chem. C* **2009**, *113*, 13139−13150.
(57) Zhang, Z. H.; Wang, Y.; Qi, Z.; Zhang, W. H.; Qin, J. Y.; Frenzel, J. *J. Phys. Chem. C* **2009**, *113*, 12629−12636.
(58) Snyder, J.; Asanithi, P.; Dalton, A. B.; Erlebacher, J. *Adv. Mater.* **2008**, *20*, 4883−+.
(59) Lang, X. Y.; Guo, H.; Chen, L. Y.; Kudo, A.; Yu, J. S.; Zhang, W.; Inoue, A.; Chen, M. W. *J. Phys. Chem. C* **2010**, *114*, 2600−2603.
(60) Xu, C. X.; Wang, R. Y.; Chen, M. W.; Zhang, Y.; Ding, Y. *Phys. Chem. Chem. Phys.* **2010**, *12*, 239−246.
(61) Tammann, G. *Z. Anorg. Allg. Chem.* **1919**, *107*, 1−239.
(62) Masing, G. *Naturwissenschaften* **1923**, *11*, 413−422.
(63) Dursun, A.; Pugh, D. B.; Corcoran, S. G. *J. Electrochem. Soc.* **2005**, *152*, B65−B72.
(64) Dursun, A.; Pugh, D. V.; Corcoran, S. G. *Electrochem. Solid State Lett.* **2003**, *6*, B32−B34.
(65) Dursun, A.; Pugh, D. V.; Corcoran, S. G. *J. Electrochem. Soc.* **2003**, *150*, B355−B360.
(66) Artymowicz, D. M.; Erlebacher, J.; Newman, R. C. *Philos. Mag.* **2009**, *89*, 1663−1693.
(67) Pickering, H. W. *Corros. Sci.* **1983**, *23*, 1107−1109, 1111−1120.
(68) Erlebacher, J. *J. Electrochem. Soc.* **2004**, *151*, C614−C626.
(69) Erlebacher, J.; Aziz, M. J.; Karma, A.; Dimitrov, N.; Sieradzki, K. *Nature* **2001**, *410*, 450−453.
(70) Kolluri, K.; Demkowicz, M. J. *Acta Mater.* **2011**, *59*, 7645−7653.
(71) Rosner, H.; Parida, S.; Kramer, D.; Volkert, C. A.; Weissmuller, J. *Adv. Eng. Mater.* **2007**, *9*, 535−541.
(72) Sun, Y.; Balk, T. J. *Scr. Mater.* **2008**, *58*, 727−730.
(73) Okman, O.; Lee, D.; Kysar, J. W. *Scr. Mater.* **2010**, *63*, 1005−1008.
(74) Jin, H. J.; Parida, S.; Kramer, D.; Weissmuller, J. *Surf. Sci.* **2008**, *602*, 3588−3594.
(75) Snyder, J.; Livi, K.; Erlebacher, J. *J. Electrochem. Soc.* **2008**, *155*, C464−C473.
(76) Okman, O.; Kysar, J. W. *J. Alloys Compd.* **2011**, *509*, 6374−6381.
(77) Bond, G. C.; Sermon, P. A.; Webb, G.; Buchanan, D. A.; Wells, P. B. *J. Chem. Soc., Chem. Commun.* **1973**, 444−445.
(78) Haruta, M.; Kobayashi, T.; Sano, H.; Yamada, N. *Chem. Lett.* **1987**, *16*, 405−408.
(79) Hutchings, G. J. *J. Catal.* **1985**, *96*, 292−295.
(80) Green, I. X.; Tang, W.; Neurock, M.; Yates, J. T. *Science* **2011**, *333*, 736−739.
(81) Haruta, M. *Catal. Today* **1997**, *36*, 153−166.
(82) Bond, G. C.; Thompson, D. T. *Catal. Rev.: Sci. Eng.* **1999**, *41*, 319−388.
(83) Zielasek, V.; Jürgens, B.; Schulz, C.; Biener, J.; Biener, M. M.; Hamza, A. V.; Bäumer, M. *Angew. Chem., Int. Ed.* **2006**, *45*, 8241−8244.
(84) Xu, C. X.; Su, J. X.; Xu, X. H.; Liu, P. P.; Zhao, H. J.; Tian, F.; Ding, Y. *J. Am. Chem. Soc.* **2007**, *129*, 42−43.
(85) Xu, C.; Xu, X.; Su, J.; Ding, Y. *J. Catal.* **2007**, *252*, 243−248.
(86) Wittstock, A.; Neumann, B.; Schaefer, A.; Dumbuya, K.; Kübel, C.; Biener, M. M.; Zielasek, V.; Steinrück, H.-P.; Gottfried, J. M.; Biener, J.; Hamza, A.; Bäumer, M. *J. Phys. Chem. C* **2009**, *113*, 5593−5600.
(87) Wittstock, A.; Wichmann, A.; Biener, J.; Bäumer, M. *Faraday Discuss.* **2011**, *152*, 87−98.
(88) Schaefer, A.; Ragazzon, D.; Wittstock, A.; Walle, L. E.; Borg, A.; Bäumer, M.; Sandell, A. *J. Phys. Chem. C* **2012**, *116*, 4564−4571.
(89) Fajin, J. L. C.; Cordeiro, M.; Gomes, J. R. B. *Chem. Commun.* **2011**, *47*, 8403−8405.
(90) Asao, N.; Ishikawa, Y.; Hatakeyama, N.; Menggenbateer; Yamamoto, Y.; Chen, M. W.; Zhang, W.; Inoue, A. *Angew. Chem., Int. Ed.* **2010**, *49*, 10093−10095.
(91) Haruta, M. *Chem. Rec.* **2003**, *3*, 75−87.
(92) Kosuda, K. M.; Wittstock, A.; Friend, C. M.; Bäumer, M. *Angew. Chem., Int. Ed.* **2012**, *51*, 1698−1701.
(93) Xu, B.; Haubrich, J.; Freyschlag, C. G.; Madix, R. J.; Friend, C. M. *Chem. Sci.* **2010**, *1*, 310−314.
(94) Xu, B.; Madix, R. J.; Friend, C. M. *J. Am. Chem. Soc.* **2010**, *132*, 16571−16580.
(95) Xu, B.; Liu, X.; Haubrich, J.; Madix, R. J.; Friend, C. M. *Angew. Chem., Int. Ed.* **2009**, *48*, 4206−4209.
(96) Liu, X.; Xu, B.; Haubrich, J.; Madix, R. J.; Friend, C. M. *J. Am. Chem. Soc.* **2009**, *131*, 5757−5759.
(97) Baker, T. A.; Liu, X.; Friend, C. M. *Phys. Chem. Chem. Phys.* **2011**, *13*, 34−46.
(98) Han, D. Q.; Xu, T. T.; Su, J. X.; Xu, X. H.; Ding, Y. *ChemCatChem* **2010**, *2*, 383−386.
(99) King, J. S.; Wittstock, A.; Biener, J.; Kucheyev, S. O.; Wang, Y. M.; Baumann, T. F.; Giri, S. K.; Hamza, A. V.; Bäumer, M.; Bent, S. F. *Nano Lett.* **2008**, *8*, 2405−2409.
(100) Ding, Y.; Chen, M. W.; Erlebacher, J. *J. Am. Chem. Soc.* **2004**, *126*, 6876−6877.
(101) Mathur, A.; Erlebacher, J. *Surf. Sci.* **2008**, *602*, 2863−2875.
(102) Herrero, E.; Buller, L. J.; Abruna, H. D. *Chem. Rev.* **2001**, *101*, 1897−1930.

(103) Liu, Y. F.; Krug, K.; Lin, P. C.; Chiu, Y. D.; Dow, W. P.; Yau, S. L.; Lee, Y. L. *J. Electrochem. Soc.* **2012**, *159*, D84−D90.
(104) Trasatti, S.; Petrii, O. A. *Pure Appl. Chem.* **1991**, *63*, 711−734.
(105) Huang, J. F. *Chem. Commun.* **2009**, 1270−1272.
(106) Rettew, R. E.; Guthrie, J. W.; Alamgir, F. M. *J. Electrochem. Soc.* **2009**, *156*, D513−D516.
(107) Wichmann, A.; Wittstock, A.; Bäumer, M. *unpublished results*; 2011.
(108) Steele, B. C. H.; Heinzel, A. *Nature* **2001**, *414*, 345−352.
(109) Rolison, D. R.; Long, R. W.; Lytle, J. C.; Fischer, A. E.; Rhodes, C. P.; McEvoy, T. M.; Bourga, M. E.; Lubers, A. M. *Chem. Soc. Rev.* **2009**, *38*, 226−252.
(110) Fiedler, E.; Grossmann, G.; Kersebohm, D. B.; Weiss, G.; Witte, C. In *Ullmann's Encyclopedia of Industrial Chemistry*; Wiley-VCH Verlag GmbH & Co. KGaA: Weinheim, 2000.
(111) Lang, X. Y.; Yuan, H. T.; Iwasa, Y.; Chen, M. W. *Scr. Mater.* **2011**, *64*, 923−926.
(112) Zhang, J. T.; Ma, H. Y.; Zhang, D. J.; Liu, P. P.; Tian, F.; Ding, Y. *Phys. Chem. Chem. Phys.* **2008**, *10*, 3250−3255.
(113) Lang, X. Y.; Qian, L. H.; Guan, P. F.; Zi, J. A.; Chen, M. W. *Appl. Phys. Lett.* **2011**, 98.
(114) Kudo, A.; Fujita, T.; Lang, X. Y.; Chen, L. Y.; Chen, M. W. *Mater. Trans.* **2010**, *51*, 1566−1569.
(115) Reutemann, W.; Kieczka, H. In *Ullmann's Encyclopedia of Industrial Chemistry*; Wiley-VCH Verlag GmbH & Co. KGaA: Weinheim, 2000.
(116) Chen, Y. X.; Heinen, M.; Jusys, Z.; Behm, R. J. *Angew. Chem., Int. Ed.* **2006**, *45*, 981−985.
(117) Wang, R. Y.; Wang, C.; Cai, W. B.; Ding, Y. *Adv. Mater.* **2010**, *22*, 1845.
(118) Bai, Y.; Yang, W. W.; Sun, Y.; Sun, C. Q. *Sens. Actuators, B* **2008**, *134*, 471−476.
(119) Qiu, H.; Huang, X. *J. Electroanal. Chem.* **2010**, *643*, 39−45.
(120) Wilson, R.; Turner, A. P. F. *Biosens. Bioelectron.* **1992**, *7*, 165−185.
(121) Tominaga, M.; Taema, Y.; Taniguchi, I. *J. Electroanal. Chem.* **2008**, *624*, 1−8.
(122) Vassilyev, Y. B.; Khazova, O. A.; Nikolaeva, N. N. *J. Electroanal. Chem.* **1985**, *196*, 105−125.
(123) Tominaga, M.; Shimazoe, T.; Nagashima, M.; Taniguchi, I. *Electrochem. Commun.* **2005**, *7*, 189−193.
(124) Tominaga, M.; Nagashima, M.; Nishiyama, K.; Taniguchi, I. *Electrochem. Commun.* **2007**, *9*, 1892−1898.
(125) Tominaga, M.; Shimazoe, T.; Nagashima, M.; Kusuda, H.; Kubo, A.; Kuwahara, Y.; Taniguchi, I. *J. Electroanal. Chem.* **2006**, *590*, 37−46.
(126) Shulga, O. V.; Zhou, D.; Demchenko, A. V.; Stine, K. J. *Analyst* **2008**, *133*, 319−322.
(127) Shulga, O. V.; Jefferson, K.; Khan, A. R.; D'Souza, V. T.; Liu, J. Y.; Demchenko, A. V.; Stine, K. J. *Chem. Mater.* **2007**, *19*, 3902−3911.
(128) Qiu, H. J.; Xu, C. X.; Huang, X. R.; Ding, Y.; Qu, Y. B.; Gao, P. J. *J. Phys. Chem. C* **2008**, *112*, 14781−14785.
(129) Qiu, H. J.; Xu, C. X.; Ji, G. L.; Huang, X. R.; Han, S. H.; Ding, Y.; Qu, Y. B. *Acta Chim. Sin.* **2008**, *66*, 2075−2080.
(130) Qiu, H. J.; Xu, C. X.; Huang, X. R.; Ding, Y.; Qu, Y. B.; Gao, P. J. *J. Phys. Chem. C* **2009**, *113*, 2521−2525.
(131) Wei, Q.; Zhao, Y. F.; Xu, C. X.; Wu, D.; Cai, Y. Y.; He, J.; Li, H.; Du, B.; Yang, M. H. *Biosens. Bioelectron.* **2011**, *26*, 3714−3718.
(132) Freyschlag, C. G.; Madix, R. J. *Mater. Today* **2011**, *14*, 134−142.
(133) Prime, K. L.; Whitesides, G. M. *Science* **1991**, *252*, 1164−1167.
(134) Prime, K. L.; Whitesides, G. M. *J. Am. Chem. Soc.* **1993**, *115*, 10714−10721.
(135) Rostovtsev, V. V.; Green, L. G.; Fokin, V. V.; Sharpless, K. B. *Angew Chem., Int. Ed.* **2002**, *41*, 2596.
(136) Zhu, A. W.; Tian, Y.; Liu, H. Q.; Luo, Y. P. *Biomaterials* **2009**, *30*, 3183−3188.
(137) Rodriguez, J. A.; Ma, S.; Liu, P.; Hrbek, J.; Evans, J.; Perez, M. *Science* **2007**, *318*, 1757−1760.
(138) Biener, M. M.; Biener, J.; Wichmann, A.; Wittstock, A.; Baumann, T. F.; Bäumer, M.; Hamza, A. V. *Nano Lett.* **2011**, *11*, 3085−3090.
(139) Kucheyev, S. O.; Biener, J.; Baumann, T. F.; Wang, Y. M.; Hamza, A. V.; Li, Z.; Lee, D. K.; Gordon, R. G. *Langmuir* **2008**, *24*, 943−948.
(140) Quiller, R. G.; Baker, T. A.; Deng, X.; Colling, M. E.; Min, B. K.; Friend, C. M. *J. Chem. Phys.* **2008**, *129*, 9.
(141) Feng, Q.; Wen, P. H.; Tao, Z. Q.; Ishikawa, Y.; Itoh, H. *Appl. Phys. Lett.* **2010**, 97.
(142) Diebold, U. *Surf. Sci. Rep.* **2003**, *48*, 53−229.
(143) Wichmann, A.; Wittstock, A.; Frank, C.; Biener, M.; Neumann, B.; Mädler, L.; Biener, J.; Rosenauer, A.; Bäumer, M. *ChemCatChem* **2012**, submitted.
(144) Rodriguez, J. A.; Hrbek, J. *Surf. Sci.* **2010**, *604*, 241−244.
(145) Rodriguez, J. A.; Liu, R.; Hrbek, J.; Perez, M.; Evans, J. *J. Mol. Catal., A: Chem.* **2008**, *281*, 59−65.
(146) Deutschmann, O.; Knözinger, H.; Kochloefl, K.; Turek, T. Heterogeneous Catalysis and Solid Catalysts, 1. Fundamentals. In *Ullmann's Encyclopedia of Industrial Chemistry*; Wiley-VCH Verlag GmbH & Co. KGaA: Weinheim, Germany, 2000.